

UCH-FC
MAG-B
O. 115
C. 1



FACULTAD DE CIENCIAS - UNIVERSIDAD DE CHILE

**PARTICIPACIÓN DE LA RESPUESTA A PROTEÍNAS MAL
PLEGADAS (UPR) EN LA REGENERACIÓN AXONAL LUEGO
DEL DAÑO AL NERVIO CIÁTICO DE RATÓN.**

Tesis entregada a la Universidad de Chile en
cumplimiento parcial de los requisitos para optar al grado de
Magíster en Ciencias Biológicas

Maritza Gabriela Beatriz Oñate Valenzuela

Director de Seminario de Título: Dr. Claudio Hetz Flores
Co-Director de Seminario de Título: Dr. Felipe Court Goldsmith

Marzo, 2015
Santiago – Chile





FACULTAD DE CIENCIAS - UNIVERSIDAD DE CHILE

**ROLE OF THE UNFOLDED PROTEIN RESPONSE (UPR)
IN AXONAL REGENERATION AFTER SCIATIC NERVE
INJURY IN MICE.**

Tesis entregada a la Universidad de Chile en
cumplimiento parcial de los requisitos para optar al grado de
Magíster en Ciencias Biológicas

Maritza Gabriela Beatriz Oñate Valenzuela

Director de Seminario de Título: Dr. Claudio Hetz Flores
Co-Director de Seminario de Título: Dr. Felipe Court Goldsmith

Marzo, 2015

Santiago – Chile

FACULTAD DE CIENCIAS
UNIVERSIDAD DE CHILE

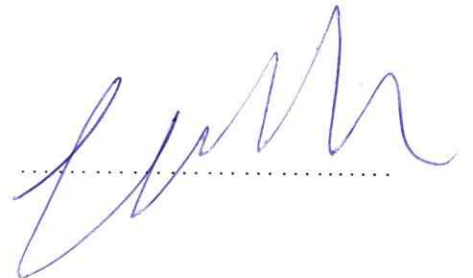
INFORME DE APROBACIÓN - TESIS DE MAGISTER

Se informa a la Escuela de Postgrado de la Facultad de Ciencias
que la Tesis de Magíster presentada por la candidata

Maritza Gabriela Beatriz Oñate Valenzuela

Ha sido aprobada por la comisión de Evaluación de la tesis como
requisito para optar al grado de Magíster en Ciencias Biológicas,
en el examen de Defensa Privada de Tesis rendido el día 26 de
Mayo del 2014.

Director de Tesis:
Dr. Claudio Hetz F.



Co-Director de Tesis:
Dr. Felipe Court G.



Comisión de Evaluación de la Tesis

Dr. Miguel Allende C.
Dr. Álvaro Glavic M.



Para mi querido Benito.

Biography



I was born on April 7, 1987 in Concepción, a place where I lived just a couple of months since then we moved with my parents to Santiago, where we settled until today. I completed my primary education at Compañía de María's school, where at age of 13 I discover what I wanted to do with my life, to be a scientist. Next year, I arrived at Pedro de Valdivia's school where I met amazing people, including my Biology teacher who encouraged me to follow the way of Science. At the end of school and sure with the plan I have decided four years ago I entered to study Molecular Biotechnology Engineering in the place that would be my second home for the following years, the Faculty of Sciences at University of Chile. During the next years I met my dear bioteks mates, with whom I shared study days, party nights and the best trips of my life. I developed my undergraduate thesis in the area of Developmental Biology, but then I decided to learn about the applied and biomedical part of the Biology and I arrived to the Laboratory of Cellular Stress and Biomedicine in the Faculty of Medicine. Also I have the opportunity to develop a thesis in collaboration with the Laboratory of Neuroscience and Glial Biology at the Catholic University. Finally, after years of hard work, I have finished successfully this thesis and I have learned a lot, personally, professionally and scientifically, determined to continue along this road.

Acknowledgements

I would like to thank to my tutors, Claudio and Felipe, to support me and encourage me to develop this project with independence and critical spirit.

To all my lab mates from U. de Chile and PUC, especially to, Vicho, René, Ute, Meli and Karen for teaching and helping me at the beginning with the experimental problems. Also, to Silke for help me with the mice colony management.

Also, I am very grateful to Moni Perez, Ale Catenaccio and Gaby Martínez, for their excellent technical expertise and with their help in the discussion and development of the experiments.

To my dears "SED" mates, for all the good times in and out of the lab, and especially to Domi for their friendship and scientific and personal support.

To my parents, Juli and Julio, for their unconditional love and support, especially to my mom, for her constant concern in every aspect of my life. To my brother and sister, Toto and Dieguito, for all the good times, the beach trips and the celebration dinners, for always listen my nerd stories, and to my dear Momo, for their love and company until the end.

Finally, I want to express my profound gratitude to my beloved husband, Jorge for sharing with me his love and interest in science, for listening and be with me in the good and bad times of this thesis, celebrating the achievements and overcoming the frustrating moments. For always be there to support me and encourage me in this process.

Index

BIOGRAPHY	v
ACKNOWLEDGEMENTS	vi
INDEX	vii
FIGURES INDEX	ix
ABBREVIATION INDEX	x
1. ABSTRACT	1
2. RESUMEN	2
3. INTRODUCTION	4
3.1 Peripheral nervous system structure	4
3.2 Wallerian degeneration and axonal regeneration in the PNS	7
3.3 ER stress and unfolded protein response (UPR)	11
3.4 The UPR in peripheral nerve injury	14
3.5 Research approach	16
4. HYPOTHESIS	17
5. OBJECTIVES	17
5.1 General Objective	17
5.2 Specific Objectives	17
6. MATERIALS AND METHODS	18
6.1 Experimental animals	18
6.2 Surgical procedures	19
6.2.1 Tunicamycin injection	19
6.2.2 Sciatic nerve injury	19
6.2.3 AAV injection in Dorsal Root Ganglia (DRG)	20
6.3 Western blot analysis	21
6.4 RNA extraction and RT-PCR	22
6.5 Locomotor function analysis	23
6.6 Electron microscopy and immunofluorescence analysis	24
6.7 Statistical analysis	25

7.	RESULTS	27
	7.1 Sciatic nerve injury triggers a local upregulation of selective UPR responses	27
	7.2 XBP1 deficiency decreases locomotor recovery, myelin removal and axonal regeneration after sciatic nerve injury	32
	7.3 Ablation of ATF4 does not affect Wallerian degeneration and locomotor recovery after nerve injury	35
	7.4 Overexpression of XBP1s in the nervous system accelerates myelin removal, axonal regeneration and locomotor recovery after nerve injury	37
	7.5 XBP1 modulates macrophage infiltration after sciatic nerve injury	39
	7.6 Local XBP1s gene transfer to DRGs enhances axonal regeneration after peripheral nerve damage	42
8.	DISCUSSION	45
9.	CONCLUSIONS	52
10.	REFERENCES	54
11.	SUPPLEMENTARY DATA	61

Figures Index

Figure 1	Organization of the spinal nerve in the PNS	5
Figure 2	Mechanism of Wallerian degeneration after peripheral nerve injury	10
Figure 3	ER stress and UPR signaling pathways	13
Figure 4	Experimental designs	26
Figure 5	Unfolded protein response is activated after sciatic nerve injury	30
Figure 6	Locomotor recovery in wild-type mice after sciatic nerve injury	31
Figure 7	XBP1 deficiency decreases myelin removal, axonal regeneration and locomotor recovery after sciatic nerve injury	34
Figure 8	ATF4 deficiency does not affect Wallerian degeneration after peripheral nerve injury	36
Figure 9	Overexpression of XBP1s increases myelin removal, axonal regeneration and locomotor recovery after peripheral nerve injury	38
Figure 10	XBP1 deficiency decreases macrophage infiltration after sciatic nerve injury	40
Figure 11	Overexpression of XBP1s increases recruitment of macrophages after injury	41
Figure 12	XBP1s overexpression in neurons enhances axonal regeneration <i>in vivo</i>	44
Figure S1	Pharmacological UPR activation in sciatic nerve	61
Figure S2	Sciatic nerve damage triggers UPR activation	62
Figure S3	<i>Cre</i> , <i>Xbp1Δ</i> and <i>Xbp1s</i> mRNA expression in XBP1 ^{Nes^{-/-}} and Tg ^{XBP1s} mice, respectively	63
Figure S4	Overexpression of XBP1s increases myelin removal and axonal regeneration at 11 days after injury.	64

Abbreviation Index

AAV	Adeno-associated virus
ATF4	Activating transcription factor 4
ATF4 ^{-/-}	ATF4 null-mice
ATF6	Activating transcription factor 6
C	Contralateral nerve
CHOP	C/EBP homologous protein
CNS	Central nervous system
D	Distal fragment from injury
dpi	Days post-injury
DMSO	Dimethyl sulfoxide
DRG	Dorsal root ganglia
EGFP	Enhanced green fluorescent protein
eIF2 α	Eukaryotic translation initiation factor 2 alpha
EM	Electron microscopy
ER	Endoplasmic reticulum
ERAD	ER-associated degradation
hpi	Hours post-injury
IRE1 α	Inositol-requiring enzyme-1 alpha
L3	Lumbar vertebrae 3
L4	Lumbar vertebrae 4
M	Medial fragment (injury region)
MBP	Myelin basic protein
Non-Tg	Control XBP1 mice (from Tg ^{XBP1s} colony)
NF-M	Neurofilament medium chain

P	Proximal fragment from injury
P0	Protein 0
PDI	Protein disulfide isomerase
PERK	PKR-like endoplasmic reticulum kinase
PL	Print length
PMP22	Peripheral myelin protein 22
PNS	Peripheral nervous system
qPCR	Quantitative real time PCR
RAGs	Regeneration-associated genes
RE	Reticulo endoplasmico
RT	Room temperature
SCI	Spinal cord injury
SFI	Sciatic functional index
Tg^{XBP1s}	XBP1s transgenic mice
Tm	Tunicamycin
TS	Toe spread
UPR	Unfolded protein response
WT	Wild-type
XBP1	X-Box-binding protein 1
XBP1^{fl/fl}	Control XBP1 mice (from XBP1 ^{Nes-/-} colony)
XBP1^{Nes-/-}	Conditional XBP1 knockout mice
XBP1s	Spliced x-Box binding protein-1
XBP1u	Unspliced x-Box binding protein-1

1. Abstract

Peripheral nerve injuries triggers the process of Wallerian degeneration distal to the injury zone, characterized by axonal degeneration, removal of myelin and axonal debris by Schwann cells and macrophages recruited into the damaged region. After this, a process of axonal regeneration initiates in the proximal stump, where new regenerated fibers extend and reinnervate their targets leading to locomotor recovery. Accumulating evidence indicate that organelle function, in particular the endoplasmic reticulum (ER) is altered after nerve damage. Alterations to ER proteostasis generate a stress condition that engages an adaptive mechanism known as the unfolded protein response (UPR) in order to restore cellular function. However, the impact of the UPR to peripheral nerve damage remains poorly explored. Here, we investigated the possible role of the UPR in the tissular changes after peripheral nerve damage and its impact in peripheral nerve regeneration. Here we demonstrated that damage triggers a specific activation of the IRE1 α /XBP1 branch but not the PERK/ATF4 axis after injury. The functional contribution of the UPR in axonal regeneration and locomotor recovery after sciatic nerve injury was assessed using mice models with specific ablation of key UPR components, including the transcriptional factors XBP1 and ATF4. Importantly, XBP1 ablation led to a significant impairment of locomotor recovery after nerve crush, but in contrast, no changes in recovery rate were detected in ATF4-null animals. The functional impairment in XBP1 knockout mice was associated with a reduced amount of regenerated axons and myelin removal, and a decrease in macrophage infiltration in the injury region. Remarkably, overexpression of XBP1s led to an increase in locomotor recovery, associated with an increased in macrophage recruitment, faster myelin

clearance and enhanced axonal regeneration. Furthermore, local overexpression of XBP1s to sensory neurons of the dorsal root ganglia using a gene transfer strategy with adeno-associated viruses (AAV) also enhanced axonal regeneration, demonstrating an important role of UPR activation in the neuronal-autonomous process of axonal regeneration after sciatic nerve injury. Our results demonstrate for the first time a functional role of specific components of the ER proteostasis network in the tissular changes associated to regeneration and functional recovery after peripheral nerve injury.

2. Resumen

La lesión a un nervio periférico desencadena un proceso denominado degeneración *Walleriana* en la región distal al sitio de daño. Este proceso está caracterizado por la degeneración del axón, la remoción de los restos de mielina y de axón por parte de las células de Schwann y macrófagos que infiltran en la zona de daño. Posteriormente, ocurre un proceso de regeneración axonal en la zona proximal a la lesión, de donde se extienden las fibras regeneradas que finalmente reinervarán el tejido blanco, permitiendo una recuperación funcional exitosa. Existe evidencia que indica que la función de organelos subcelulares, y en particular del retículo endoplásmico (RE), se ven alterados luego de un daño a un nervio. Alteraciones a la proteostasis del RE generan una condición de estrés que desencadena un mecanismo adaptativo conocido como la respuesta a proteínas mal plegadas (UPR por sus siglas en inglés) que contribuye a restaurar la función celular. Sin embargo, el impacto de la

UPR luego de un daño al nervio periférico aún es desconocido. En este estudio investigamos el posible papel funcional de la UPR sobre los cambios tisulares locales luego del daño y el impacto que tiene sobre la regeneración axonal periférica. Demostramos que el daño al nervio ciático desencadena la activación específica de la rama de la UPR mediada por IRE1 α /XBP1 y no de la vía PERK/ATF4 luego del daño. Para evaluar la contribución funcional de la UPR en la regeneración axonal y recuperación locomotora luego del daño, utilizamos modelos murinos deficientes de dos componentes claves de la UPR, los factores de transcripción XBP1 y ATF4. La eliminación genética de XBP1 en el sistema nervioso produjo un retraso en la recuperación locomotora luego del daño. Sin embargo, no se observaron cambios en la recuperación funcional en los animales nulos para ATF4. El efecto funcional en los ratones deficientes para XBP1 estuvo asociado a una menor cantidad de axones regenerados, una disminución en la remoción de mielina y una baja infiltración de macrófagos a la zona de daño. Por otro lado, la sobreexpresión de la forma activa de XBP1 en neuronas y glías produjo un aumento en la recuperación locomotora, asociado a un aumento en la remoción de mielina, un mayor número de axones regenerados y un aumento en la infiltración de macrófagos. Además, el tratamiento de ratones silvestres con virus adeno-asociados en las neuronas sensitivas que inervan al nervio ciático, para expresar la forma activa de XBP1, provocó un aumento en la regeneración axonal, demostrando un importante papel de la activación autónoma-neuronal de la UPR en la regeneración axonal luego del daño al nervio ciático. Nuestros resultados sugieren un papel clave de los componentes de la proteostasis del RE en los cambios tisulares asociados a la regeneración axonal y a una recuperación funcional exitosa.

Omate
Valenzuela

3. Introduction

3.1 Peripheral nervous system structure

The peripheral nervous system (PNS) is the region of the nervous system composed by peripheral nerves and ganglia outside the brain and spinal cord. The cranial and spinal nerves conduct impulses from the central nervous system (CNS) to the periphery as well as sensory input toward the CNS. In the PNS, neuronal somas are located in structures known as ganglia outside the CNS. Two principal cell types form the PNS, neurons and glial cells. Neurons are categorized in sensory and motoneurons. Sensory neurons transmit impulses from peripheral receptors to the CNS, and their somas are located in dorsal root ganglia (DRG) located in pairs outside each vertebral segment of the spinal cord and their axons project both to the PNS and CNS through spinal nerves. Motoneurons transmit impulses from the CNS to effectors cells. These neurons are located along the ventral horn of the spinal cord and project to spinal nerves through the ventral roots, in the case of the somatic nervous system (Fig 1A and B), and project their axons from the spinal cord in the case of the pre-ganglionic neuron, and form the paravertebral ganglia, in the case of the postganglionic neuron of the autonomic nervous system (White et al, 1952).

Schwann cells are the principal glial cell component in the PNS and are involved in several processes including transmission of the action potential, guidance of growing peripheral axons, clearance of debris after injury, production of extracellular matrix and modulation of neuromuscular synapses (Toy & Namgung, 2013; Pereira et al, 2012).

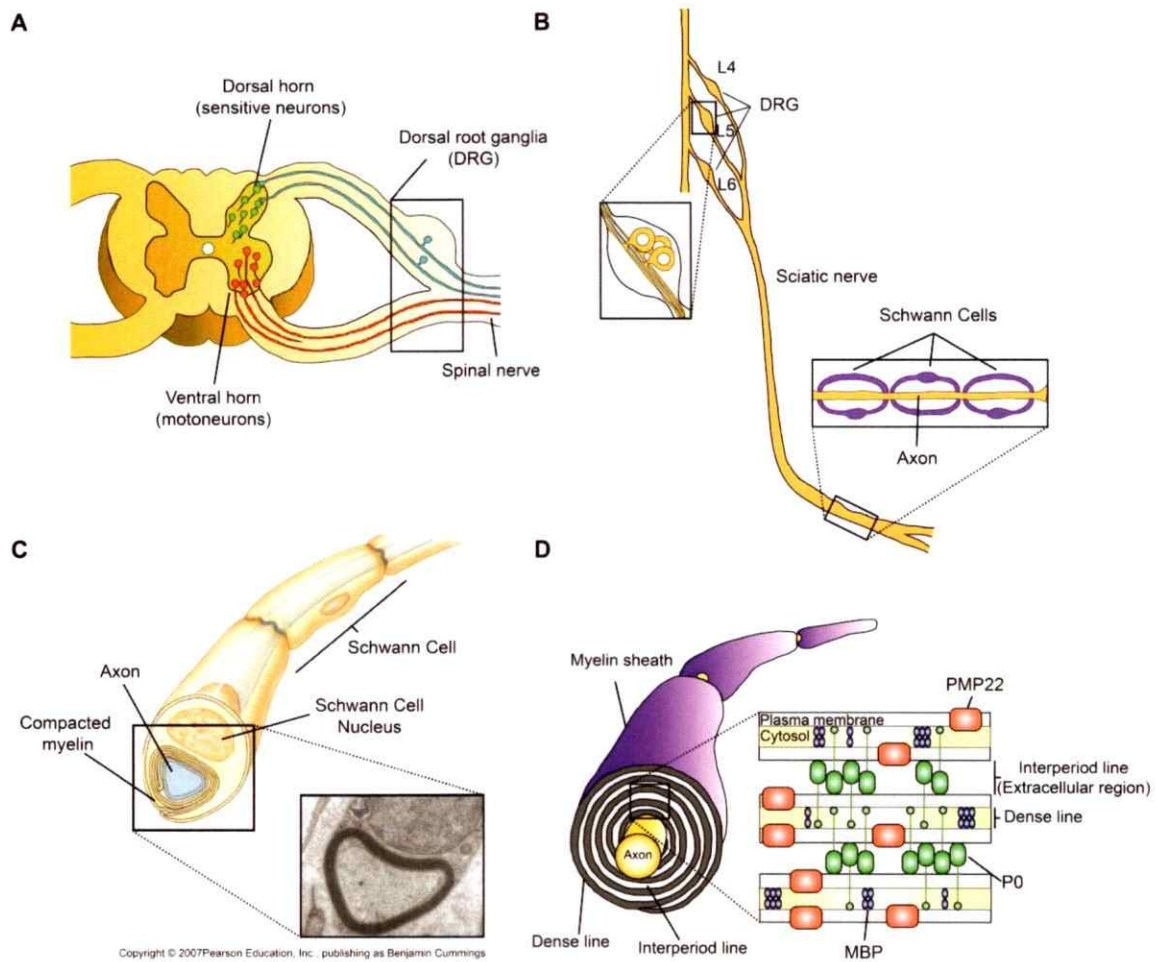


Figure 1. Organization of the spinal nerve in the PNS. (A) Diagram of a spinal cord section showing motoneurons (red) located in the ventral horn projecting to the spinal nerve and sensory neurons (blue) located in the dorsal root ganglion, DRG (box) projecting to the dorsal horn in the spinal cord and to the peripheral spinal nerve. **(B)** Scheme of the sciatic nerve showing sensitive neurons cell bodies from DRG of lumbar vertebrae L4, L5 and L6 and peripheral axon surrounded by Schwann cells. **(C)** Cartoon of a peripheral nerve and an electron microscope image showing the compact myelin surrounding the axon. **(D)** Peripheral axon (yellow) surrounded by a myelin sheath (purple) produced by the Schwann cell. The inset shows the molecular structure of myelin, including MBP, P0 and PMP-22.



During development, Schwann cells originate from neural crest-derived precursors and migrate along growing axons, which promote trophic, mitogenic and differentiation effects on precursor cells. Then, Schwann cells extend processes to sort large individual caliber axons to form myelinating fibers, and associate multiple small axons to form non-myelinating fibers termed Remak bundles. Myelinating and Remak Schwann cells differ not just in their morphological relationship to the axon, rather, they are fundamentally distinct, characterized by expression of different transcription factors, proteins and lipids. Most peripheral nerves consist of a mixture of myelinated and Remak fibers (Salzer, 2012).

Each Schwann cell covers an axon of motor or sensitive neurons to form the myelin sheath. This structure is a flattened extension of the Schwann cell that elongates and repeatedly encircles the axon forming layers that are compacted together (Fig 1C). In the compact myelin, it is possible to distinguish the major dense line, a thin layer of cytoplasm bound by cell membrane, and the interperiod line, the extension of the extracellular space between these cellular components (Fig 1D). The myelin sheath is predominantly composed of cholesterol and sphingolipids, but certain proteins also play a significant role in its structure. Protein 0 (P0) is a glycoprotein that accounts for over a half of the total protein present in the compact PNS myelin and forms the interperiod line by linking its immunoglobulin G (IgG)-like extracellular domains to form a complex lattice (Quarles, 2002). Myelin basic protein (MBP) is a cytoplasmatic protein that forms the major dense line of compact myelin. An additional glycoprotein, peripheral myelin protein 22 (PMP22), constitutes 2-5% of total protein mass and participates in the adhesion of apposing membranes for the maintenance of the compacted myelin sheath (Fig 1D). The impact of these proteins on myelin structure is underscored by the severe

consequences of altering their expression or point mutations in its aminoacidic structure, which triggers accumulation of this proteins in the Schwann cell leading to severe demyelinating neuropathies (Han et al, 2013; Quarles, 2002).

3.2 Wallerian degeneration and axonal regeneration in the PNS

Injury to peripheral nerves results in loss of motor and sensory functions. Damaged fibers distal to the lesion are disconnected from the neuronal body and undergo a process known as Wallerian degeneration (Waller, 1850). In the PNS, this process promotes a microenvironment that allows axonal regrowth, and elongation from the proximal stump. The functional significance of axonal regeneration is to replace the degenerated segment, favoring re-innervation of target organs and restitution of their functions (Allodi et al, 2012).

Wallerian degeneration is a tissular reaction initiated distal to the injury site. This process is characterized by a marked increased in calcium into the axon from extracellular and intracellular stores. Calcium influx leads to the activation of calpains, proteases which are capable of cleave axonal neurofilaments and microtubule-associated components. These proteins induce cytoskeleton breakdown and axonal fragmentation during the first 48 hours, leading to axonal degeneration (Wang et al, 2012; Court & Coleman, 2012).

Axonal degeneration also leads to loss of contact between axons and Schwann cells, triggering Schwann cell dedifferentiation and posterior proliferation around 3 days after injury (Fig 2B). The reaction of Schwann cells to nerve injury includes profound

changes in gene expression leading to a dedifferentiated phenotype (Vargas & Barres, 2007). In the case of myelinating cells this changes involves a balance between two opposing transcriptional programs, a group of cell-intrinsic transcription factors, including Krox-20, Sox-10, Oct-6 and NFκ-B, which regulates positively the myelination process and the activation of another group of factor, which are described as negative transcriptional regulators of myelination such as c-Jun, Notch, Sox-2, Id2, Pax-3, Krox-24 and Egr-3. In addition, a large number of genes related to myelination are down regulated, including enzymes that provide for cholesterol synthesis, structural proteins such as P0, MBP, and membrane associated proteins such as myelin associated glycoprotein (MAG) and periaxin. This switch-off is accompanied by the upregulation of another group of molecules, most of which are normally found on immature cells prior to myelination. This includes L1 and NCAM, p75 low affinity neurotrophin receptor (p75NTR) and glial fibrillary acidic protein (GFAP) (Jessen & Mirsky, 2008; Arthur-Farraj et al, 2012).

Schwann cells also participate actively in both breakdown of the myelin sheath and the clearance of axonal and myelin debris. During the first days post injury, Schwann cells are able to segment their myelin sheaths, forming myelin ovoids (Hirata & Kawabuchi, 2002). At early stages of degeneration, Schwann cells secrete cytokines and chemokines that stimulate the recruitment of immune cells, principally macrophages, into the injured region contributing to the removal of myelin debris at late stages (Fawcett & Keynes, 1990; Gaudet et al, 2011; Glen & Talbot, 2013).

Macrophages are recruited to the injured region between 5 and 7 days post-injury (dpi) and reach the maximal infiltration at 14 dpi, leading to a fast clearance of myelin debris (Fig 2C; Bruck, 1997). Efficient removal of myelin appears to be one of

the most important requirements for successful axonal regeneration after peripheral nerve injury, due to the presence of myelin-associated growth inhibitors factors (Duvobý, 2011; Gaudet et al, 2011).

The onset of regeneration is also associated with the expression of specific genes and proteins in the injured neuron. The genes upregulated during the regeneration process are denominated regeneration-associated genes (RAGs) and several of them are also those associated with axonal growth during development (Fancy et al, 2011). In addition, Schwann cells favor regeneration by providing structural guidance and growth-promoting substrates to regenerating axons. After injury, Schwann cells begin to proliferate and align in endoneural tubes known as bands of Bungner, which guide the extending fibers (Allodi et al, 2012). Regenerating axons grow in close association with these Schwann cell bands along their original pathways to reinnervate their targets (Fawcett & Keynes, 1990). Also, Schwann cells secrete trophic factors to promote the extension of regenerated axons (Madduri & Gander, 2010). Once the regenerating axons are extended, Schwann cells change their gene expression pattern to re-differentiate again. Upregulation of myelin-associated genes allows Schwann cells to remyelinate the new regenerated fibers in order to reestablish glial function. Finally, regenerated fibers successfully reach their targets allowing a fully successful locomotor recovery (Fig 2D).

Together, these tissular changes promote a permissive environment for efficient axonal regeneration in the PNS (Chen et al, 2007). On the contrary, after CNS injury, axonal degeneration proceeds but the clearance of myelin debris is limited and oligodendrocytes die by apoptosis. In addition, reactive astrocytes, form the glial scar

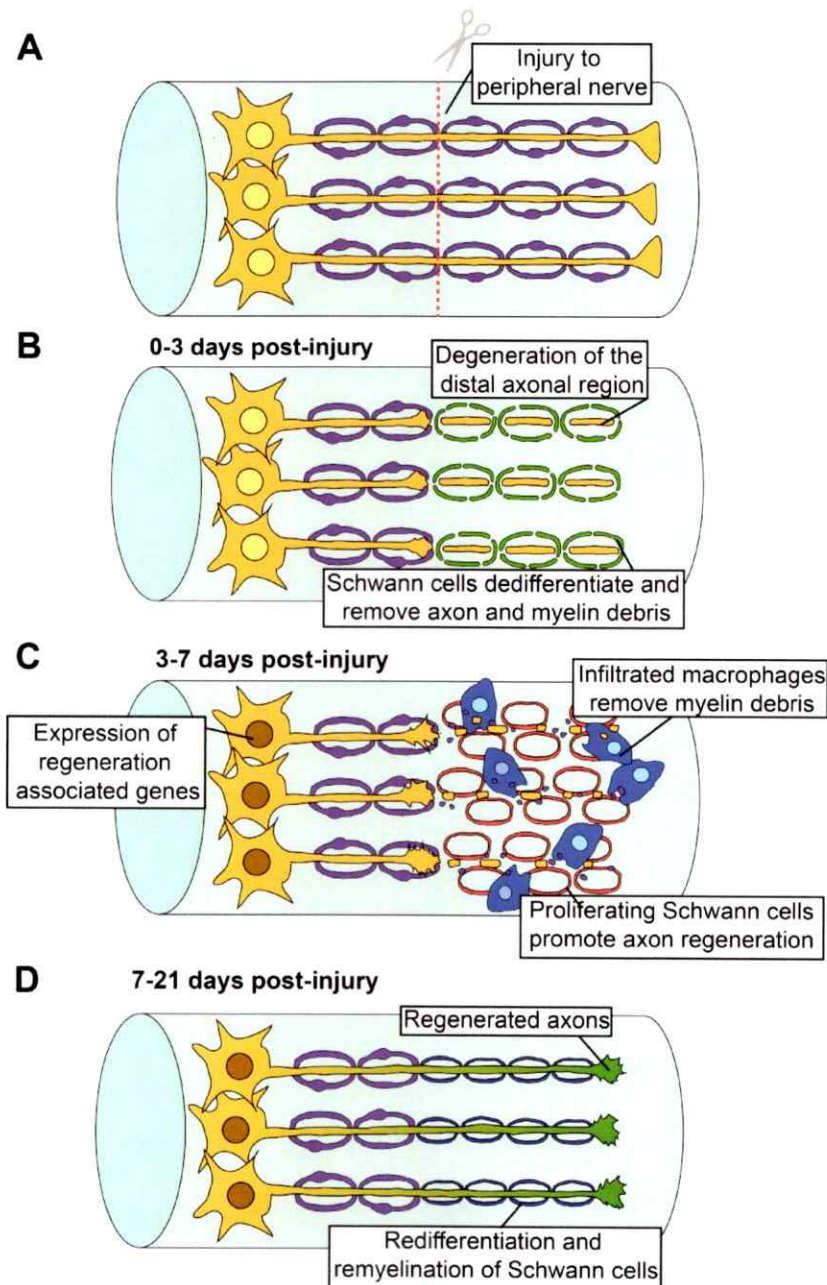


Figure 2. Mechanism of Wallerian degeneration after peripheral nerve injury. (A) After injury to peripheral nerve, distal region disconnected from neuronal somas degenerate. (B) During the first 3 dpi axonal cytoskeleton disintegrates causing fragmentation. Schwann cells dedifferentiate and play an early role in clearance of myelin sheath and axonal debris. (C) In the next 3 to 7 dpi Schwann cells proliferate, secreting trophic factors to promote axonal growth, and cytokines and chemokines to stimulate infiltration of immune cells, principally macrophages to the injury region, which remove the remained myelin and axonal debris. Local response also is supported by an autonomous neuronal component. Expression of RAGs promotes axonal extension. (D) Finally, between 7 and 21 dpi, efficient clearance of axonal debris and inhibitory factors of myelin and stimulation of axonal growth determinates axonal regeneration leading to redifferentiation of Schwann cells, remyelination of the regenerated fibers, reinnervation to their targets and successful locomotor recovery.

and secrete growth-inhibitory molecules (Barrette et al, 2008), generating an unfavorable environment for axonal regeneration (Vargas & Barres, 2007; Sofroniew, 2009; Gaudet et al, 2011; Ferguson & Son, 2011; Toy & Namgung, 2013). Therefore, the cellular and tissular reaction to local stress condition, will partially determine the regenerative capability of a damage neuron and therefore the functional outcome (Allen & Barres, 2009; Lutz & Barres, 2014).

3.3 ER stress and unfolded protein response (UPR)

Alterations to organelle function, in particular the endoplasmic reticulum (ER) and mitochondria, have been observed after damage in both the neuronal cell body and its axon. Our laboratory had recently reported that local release of calcium from the ER in damaged axons (Villegas et al, 2014) and the downstream activation of the mitochondrial transition pore (Barrientos et al, 2011) are central components of the axonal destruction program. Accumulating evidence indicate that ER proteostasis is altered after PNS or CNS injury, generating a protein folding stress reaction in both neurons and glial cells (Li et al, 2013). The ER is a dynamic and interconnected tubular network that spans through the neuronal cell body, dendrites and axons (Ramírez & Couve, 2011; Villegas et al, 2014), contributing to the modulation of calcium-mediated signaling, protein folding, secretion, and the biosynthesis of lipids. ER stress engages an adaptive reaction known as the unfolded protein response (UPR) that operates as a mechanism to restore cellular proteostasis (Walter and Ron, 2011).

In the first place, the UPR increases the protein folding capacity of the ER upregulating the expression of several chaperones, such as BiP, calreticulin, calnexin

and protein disulfide isomerase (PDI) proteins (ERp57, ERp72 and PDI). Moreover, the UPR increases the expression of genes involved in quality control, protein degradation via ER-associated degradation (ERAD) and autophagy (Schroder and Kaufman, 2005). When the adaptive mechanisms are insufficient to recover homeostasis, or when ER stress is chronic and irreversible, activation of the UPR also leads to cell death by apoptosis (Urrea et al, 2013).

The UPR is initiated by the activation of three ER transmembrane proteins that operate as stress sensors (Fig 3) (Hetz, 2012). The most conserved UPR sensor is Inositol-Requiring Enzyme-1 alpha (IRE1 α), an ER-located kinase and ribonuclease that splice-out a 26 nucleotide intron of the mRNA encoding the transcription factor X-box Binding Protein-1 (XBP1) (Shen et al, 2001; Yoshida et al, 2001; Calfon et al, 2002; Lee et al, 2002). This processing event shifts the coding reading frame of the mRNA, leading to the synthesis of an active transcription factor known as XBP1s that controls the expression of a subset of UPR-target genes involved in protein folding, ERAD, phospholipid synthesis, among other processes (Lee et al, 2003; Acosta-Alvear et al, 2007). However, the universe of XBP1s target genes depends on the cell type affected and the stimuli involved (Hetz et al, 2011). IRE1 α also engages other signaling events through the binding of adapter proteins, in addition to control the stability of certain mRNAs and miRNAs (Maurel et al, 2014).

Other UPR effects are mediated by the stress sensor protein kinase (PKR)-like endoplasmic reticulum kinase (PERK), which inhibits general protein translation through the inactivation of the eukaryotic translation initiation factor 2 α (eIF2 α) by phosphorylation, alleviating ER stress by decreasing the overload of misfolded proteins

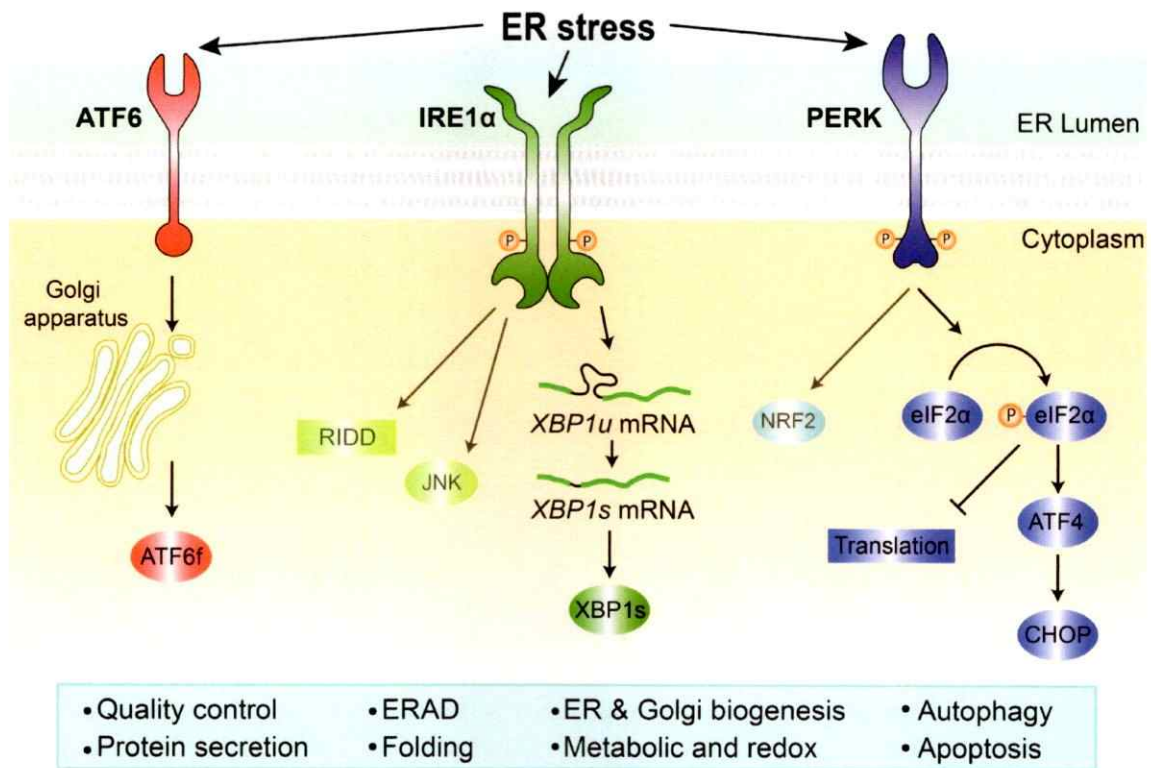


Figure 3. ER stress and UPR signaling pathways. The accumulation of misfolded proteins in the ER leads to the activation of the adaptive stress response known as the UPR through three sensors: IRE1 α , ATF6 and PERK, which triggers signaling cascades to restore cellular homeostasis or to activate the pathway of cell death by apoptosis. Activation of IRE1 α controls the processing of the mRNA encoding XBP1, a transcription factor that upregulates many essential UPR genes involved in folding, organelle biogenesis, ERAD, autophagy, and protein quality control. Activation of PERK decreases the general protein synthesis rate through phosphorylation of the initiation factor eIF2 α . In contrast, this protein increases the specific translation of the ATF4 mRNA, which encodes a transcription factor that induces the expression of genes involved in amino acid metabolism, autophagy, antioxidant responses, and apoptosis. ATF6 is a type II ER transmembrane protein encoding a bZIP transcriptional factor in its cytosolic domain that is localized at the ER in unstressed cells. Upon ER stress induction, ATF6 is processed at the Golgi apparatus, releasing its cytosolic domain, which then translocates to the nucleus where it increases the expression of some ER chaperones, ERAD-related genes.

(Harding et al, 2000). However, eIF2 α phosphorylation triggers the specific translation of selective mRNAs where the most studied is the activating transcription factor 4 (ATF4), which is essential for the upregulation of redox status, protein metabolism and autophagy (Harding et al, 2003; Walter & Ron, 2011). However, under sustained or chronic ER stress ATF4 activates a pro-apoptotic program mediated in part by the upregulation of CCAAT/Enhancer-Binding Protein (C/EBP, CHOP), BCL-2 family members, and the enhancement of oxidative stress (Tabas & Ron, 2011). Another UPR pathway is mediated by activating transcription factor 6 (ATF6), this protein is synthesized as an inactive precursor, retained at the ER by a transmembrane spanning segment. Under ER stress conditions, ATF6 translocates to the Golgi where it is processed, first by site-1 protease and then in an intramembrane region by site-2 protease. This proteolytic processing releases its cytoplasmic domain, ATF6f (a fragment of ATF6), which operates as a transcriptional activator that upregulates many UPR genes related to ERAD and protein folding, among other processes (Haze et al, 1999; Chen et al, 2002; Shoulders et al, 2013). Overall, the UPR integrates information about the intensity and duration of the stress stimuli to determine cell fate toward recovering proteostasis or eliminating damaged cells by apoptosis.

3.4 The UPR in peripheral nerve injury

ER stress is emerging as a relevant factor driving both neurodegeneration and cell survival on a context-specific manner as reported for the most common brain diseases (Hetz & Mollereau, 2014). Mechanical injury to the CNS has been shown to engage an ER stress reaction, possibly having detrimental consequences to motor

recovery (Li et al, 2013). We have recently reported that the UPR is rapidly activated along the spine a few hours after spinal cord injury (SCI), and is maintained for several days (Valenzuela et al, 2012). Genetic ablation of ATF4 or XBP1 dramatically reduced locomotor recovery after SCI, whereas local delivery of XBP1s to the injury zone improved oligodendrocyte survival and enhanced locomotor recovery (Valenzuela et al, 2012). Other studies have also proved a functional impact of the UPR after SCI using genetic or pharmacological manipulation of the pathway (see examples in Ohri et al, 2012, 2013, 2014; Zhang et al, 2013, 2014). In contrast, only a few correlative reports are available linking ER stress with peripheral nerve damage. For example, distal sciatic nerve injury triggers a transient ER stress response in ventral horn motoneuron, and spine root avulsion generates a stronger UPR reaction in the same neuronal population (Saxena et al, 2009; Penas et al, 2011). A functional study suggested that overexpression of the ER chaperone BiP can increase the survival of root-avulsed motoneurons (Penas et al, 2011). In the nerve, Schwann cells also upregulate BiP expression after sciatic nerve injury during their dedifferentiation process (Mantuano et al, 2011). *In vitro* studies demonstrated that the eIF2 α /CHOP axis is a central mediator of apoptosis in Schwann cell exposed to pro-inflammatory signals (Mantuano et al, 2011). Furthermore, in models of Charcot-Marie-Tooth-1B disease, a pathology involving the misfolding and ER-retention of a mutated form of the P0 myelin glycoprotein, genetic targeting of *Chop* fully rescues motor deficits and reduced demyelination (Pennuto et al, 2008; D'Antonio et al, 2013). Similarly, ER stress has been implicated in other myelin-related disorders affecting oligodendrocytes such as multiple sclerosis and Pelizaeus-Merzbacher disease (Lin & Popko, 2009). Nevertheless, the functional contribution of ER stress to the degenerative and regenerative process observed after peripheral nerve injury remains to be determined,

and direct manipulation of proximal UPR components is required to address this essential question.

3.5 Research approach

Despite the evidence demonstrating an early activation of UPR in neuronal cell bodies and Schwann cells after peripheral nerve injury, the role of the UPR in axonal degeneration and their contribution to the regenerative response and functional recovery after nerve damage has not been studied so far.

In this study, using genetic manipulation of the UPR, we have systematically investigated the impact of targeting the pathway in the tissular changes that follows a peripheral nerve injury and its impact in peripheral nerve regeneration. We evaluated the upregulation of two UPR branches at different times post-injury in the sciatic nerve to characterized UPR kinetic in the injury zone and in adjacent regions. To evaluate the functional contribution of the UPR to axonal regeneration, locomotor recovery was assessed after sciatic nerve injury in models of loss and gain-of-function for key UPR components. Furthermore, to determine the specific cell-types responding to ER stress during axonal regeneration, we have developed a gene therapy strategy to deliver the active form of XBP1 in sensitive neurons using AAV. Our general aim is to determine the possible functional contribution of the UPR after peripheral nerve injury to axonal regeneration and locomotor recovery. We plan to identify specific components of the proteostasis network that may operate as possible therapeutic targets for the future treatment to peripheral neuropathies and neurodegenerative conditions in the PNS or CNS.

4. Hypothesis

The activation of the unfolded protein response (UPR) is involved in the process of Wallerian degeneration, promoting axonal regeneration and locomotor recovery after peripheral nerve injury.

5. Objectives

5.1 General Objective

To study the possible contribution of specific components of the unfolded protein response to axonal regeneration and locomotor recovery after sciatic nerve injury.

5.2 Specific Objectives

1. To characterize the activation of ER stress markers and UPR signaling components in the sciatic nerve after injury.
2. To determine the rate of locomotor recovery of ATF4 deficient animals and a conditional XBP1 knockout mice, in addition to an XBP1 transgenic mice in the nervous system.
3. To define and compare the possible effects of the genetic manipulation of the UPR after sciatic nerve injury in the extent of axonal degeneration, myelin removal and axonal regeneration responses after sciatic nerve injury.
4. To assess the contribution of UPR in the intrinsic neuronal mechanism of axonal regeneration.

6. Materials and Methods

6.1 Experimental animals

Animals of 8 weeks of age, with body weight between 20 and 25 g, were kept under standard conditions of light and temperature and feed with food and water *ad libitum*. XBP1 conditional knockout mice (XBP1^{Nes^{-/-}}) and ATF4 full knockout mice (ATF4^{-/-}) have been previously described (Hetz et al, 2008; Masuoka & Townes, 2002). Briefly, for the generation of XBP1^{Nes^{-/-}} mice, XBP1^{fl^{ox}/fl^{ox}} mice were crossed with animals expressing the Cre recombinase under the control of the Nestin promoter to specifically delete *xbp1* in the nervous system. The ATF4^{-/-} mice were generated by crossing heterozygous mice and the model was generated by replacing 2 exons that constitute the entire ATF4 coding region after the first codon, as well as the polyadenylation signal with the neomycin phosphotransferase gene. To generate the XBP1s transgenic mice (Tg^{XBP1s}), the mouse XBP1s cDNA was subcloned into the Xho1 site of the MoPrP.Xho vector (Borchelt et al, 1996) to drive XBP1s expression by the PrP promoter in the nervous system. The plasmid was linearized and microinjected into CBA-C57BL/6 mouse-derived pronuclei of fertilized oocytes using standard assays. The presence of the transgene was confirmed by PCR of genomic DNA from the tail (forward primer: 5'-ACACGCTTGGGAATGGACAC-3'; reverse: 5'-CCATGGGAAGATGTTCTGGG-3'). Line 3 was used in this study based on the intensity and tissue-specificity of the expression of the transgene after comparative analysis (Centro de Estudios Científicos, Valdivia, Chile). The founder line was then backcrossed onto the C57BL/6 background for more than 15 generations to obtain the experimental group (Non-Tg and Tg^{XBP1s} mice) (PhD thesis, Gabriela Martínez, unpublished).

6.2 Surgical procedures

6.2.1 Tunicamycin injection

For tunicamycin (Tm) treatments, animals were intraperitoneally injected at a dose of 1 µg/g body weight of a 0.05 mg/ml suspension dissolved in 150 mM sucrose (Rodriguez et al, 2012). As control, animals were injected with a same dose of dimethyl sulfoxide (DMSO). 16 h after injection, animals were euthanized by an overdose of anesthesia (1 ml of 2-2-2 tribromoethanol 330 mg/Kg) for tissue extraction. Liver, cerebral cortex and sciatic nerve were removed for biochemical analysis.

6.2.2 Sciatic nerve injury

For sciatic nerve injury, mice were intraperitoneally injected with 330 mg/Kg 2-2-2 tribromoethanol (Sigma, St. Louis, MO, USA) and with 30 mg/Kg of Tramadol for anesthetic and analgesic treatment, respectively. Then, the right sciatic nerve was exposed at the level of the sciatic notch after surgical dissection of skin and muscle. The sciatic nerve was crushed (crush injury) three times for 5 seconds with Dumont #5 forceps (Fine Science Tools INC. CA, USA) and then skin was suture with mouse metal clips. The left sciatic nerve was subjected to the same intervention without nerve crush to use as sham control group. During recovery, mice were placed in a temperature-controlled chamber. At different days post surgery, animals were euthanized by overdose of anesthesia and the sciatic nerve and DRGs were removed for different analysis.

6.2.3 AAV injection in Dorsal Root Ganglia (DRG)

The production and quantification of recombinant AAV2.XBP1s/GFP (2.9×10^{12} DRP/ml) and control AAV2.GFP (1.22×10^{12} DRP/ml) was previously described (Valenzuela et al, 2012; Zuleta et al, 2012; Valdés et al, 2014). Briefly, the whole Xbp-1 expression cassette was excised from pcDNA3-XBP-1S and inserted into a pro-viral plasmid pAAVsp70 containing AAV2-inverted terminal repeats (ITRs). The vector also carries a GFP expression cassette that serves as a fluorescent marker for transduced cells. Recombinant AAV2.XBP1S was produced by triple transfection of 293 cells and then purified by column affinity chromatography. For DRG injection, mice were anesthetized and an incision was made in the skin just to the right of the spinous process in the dorsal midline. The muscular fascia was incised and the paraspinal muscles were separated exposing the lateral region of the right third lumbar (L3) and L4 vertebrae and the dorsal region transverse processes. To expose DRGs from L3 and L4 a right hemilaminectomy was performed to removed the transverse processes. AAV injections were performed using a 2 μ l Hamilton syringe fitted with a 34 G needle. The syringe was held in a micromanipulator. For each DRG, 1 μ l of a solution with the AAV mixed with 0.3% fast green was injected at a constant flow of 0.01 μ l/s, using a microinjector (Neurostar InjectoMate, IM1A193). After injection the wound was closed by suturing the paraspinal muscles using 4-0 polyamide monofilament non-absorbable suture and the skin was closed using mouse metal clips. 7 days after injection, the sciatic nerve was injured at the notch level. To evaluate axonal regeneration, a 3 mm segment located 3 mm distal and 6 mm proximal to the injury were removed at 14 dpi for immunohistochemical analysis.

6.3 Western blot analysis

A 5-mm sciatic nerve tissue containing the injury region (medial; M), in addition to adjacent proximal (P) and distal (D) regions of the same size were collected (Fig 4) and homogenized using a plastic Dounce homogenizer in extraction buffer (95 mM NaCl, 25 mM Tris-HCl, pH 7.4, 10 mM EDTA pH 8.0, 1% SDS, 1 mM NaF, 1mM Na₃VO₄ and 1% Protease Inhibitor Cocktail (PIC, Sigma-Aldrich, #P8340). 10µl of this buffer was used per mm of sciatic nerve. Lysates were sonicated, centrifuged at 13,000 rpm for 10 min at 4°C and then supernatant was used for protein analysis. For liver and cortex protein extraction, tissue was extracted and homogenized in RIPA buffer (20mM Tris pH 8.0, 150mM NaCl, 0.1% SDS, 0.5% DOC, 0.5% Triton X-100) containing a protease inhibitor cocktail (Roche, Basel, Switzerland). Western blot was performed using SDS-PAGE and polyvinylidene difluoride (PVDF, Pierce) membranes as previously described (Barrientos et al, 2011). The following antibodies and dilutions were used; anti-Hsp90, 1:5000 (sc-7947, H114, Santa Cruz, CA, USA), anti-BiP, 1:1000 (SPA-826, Stressgen), and anti-ERp57 1:3000 (SPA-585, Stressgen). Band intensities were normalized to Hsp90 used as a loading control. Densitometry analysis of the bands was performed using Image-J software (NIH, Bethesda, MD, USA).

6.4 RNA extraction and RT-PCR

A 5 millimeter (mm) segment of the sciatic nerve obtained 3 mm distal to injury, DRGs from L3 and L4 vertebrae and cerebellum were collected and homogenized in 600 µl of Trizol (Invitrogen, USA) for total RNA extraction using standard protocols (Fig 4). cDNA was synthesized with a High Capacity cDNA Reverse Transcription kit (Applied Biosystems). Quantitative real time PCR (qPCR) was performed using SYBR Green fluorescent reagent and an Mx3005P QPCR System (Stratagene) and the following primers: *Xbp1s* (forward: 5'-TGCTGAGTCCGCAGCAGGTG-3', reverse: 5'-GACTAGCAGACTCTGGGGAAG-3'), *Atf3* (forward: 5'-TTGACGGTAACTGACTCCAGC-3', reverse: 5'-GAGGATTTTGCTAACCTGACACC-3'), *Chop* (forward: 5'-TGGAGAGCGAGGGCTTTG-3', reverse: 5'-GTCCCTAGCTTGGCTGACAGA-3'), *Gadd34* (forward: 5'-TTACCAGAGACAGGGGTAGGT-3', reverse: 5'-GAGGGACGCCCAACTTC-3'), *Wfs1* (forward: 5'-CCATCAACATGCTCCCGTTC-3', reverse: 5'-GGGTAGGCCTCGCCAT-3'), *β-actin* (forward: 5'-CTCAGGAGGAGCAATGATCTTGAT-3', reverse: 5'-TACCACCATGTACCCAGGCA-3') and *Cre* (forward: 5'-ATCGCTCGACCAGTTTAGTT-3', reverse: 5'-CTGACGGTGGGAGAATGTTA-3'). The relative amount of mRNA was calculated by the comparative threshold cycle method with *β-actin* as control. Primer sequences were obtained from PrimerBank. XBP1 mRNA splicing assay was performed as previously described (Rodriguez et al, 2012) using PstI digestion of PCR products using the following primers: mXBP1.3S (5'-AAACAGAGTAGCAGCGCAGACTGC-3') and mXBP1.2AS: (5'-GGATCTCTAAACTAGAGGCTTGGTG-3').

6.5 Locomotor function analysis

Locomotor recovery was evaluated using the sciatic functional index (SFI) as described previously (Insera et al, 1998). Animals underwent a pre and post surgery walking track analysis. Pawprints were recorded by moistening the hindlimbs of each animal with black ink and having them walk unassisted along an 11 X 56 cm white paper corridor. Tracks were obtained before surgery (0 day), and 1, 3, 7, 9, 14 and 21 days after right nerve injury. Prints for analysis were chosen for clarity and consistency at a point when the animal was walking at a moderate pace and if necessary, mice were walked at most 3 times to obtain measurable prints. All tracks were obtained and analyzed in a blinded fashion. The tracks were evaluated for two different parameters: toe spread (TS), the distance between the first and fifth toes, and print length (PL), the distance between the third toe and the hind pad. Measurements of all parameters were made for the right injured (experimental; E) and the left control (normal; N) paw prints and the SFI were calculated according to the formula;

$$\text{SFI} = 118.9 \left(\frac{\text{ETS} - \text{NTS}}{\text{NTS}} \right) - 51.2 \left(\frac{\text{EPL} - \text{NPL}}{\text{NPL}} \right) - 7.5$$

where ETS and NTS are experimental and normal TS and EPL and NPL are experimental and normal PL, respectively.

6.6 Electron microscopy and immunofluorescence analysis

Sciatic nerves were extracted at 11 and 14 days after injury. A 3 mm region located 3 mm distal to crush site was removed for electron microscopy; the contiguous 3-mm region located 6 mm distal to injury was removed for immunofluorescence analysis (Fig 4).

For electron microscopy (EM) analysis, sciatic nerves were fixed overnight with 2.5% glutaraldehyde, 0.01% picric acid and 0.05 M cacodylate buffer, pH 7.3. Nerves were incubated in the same buffer with 1% OsO₄ for 1 h and then immersed in 2% uranyl acetate for 1 h, dehydrated in a gradient of ethanol and acetone, and infiltrated in Epon (Ted Pella) as previously described (Villegas et al, 2014). Transversal semithin and ultrathin sections were obtained using an ultramicrotome (Reichert). Thin 80 nm sections were obtained and mounted in copper grids and contrasted using 1% uranyl acetate and lead citrate. Observations of the grids were made using a Phillips Tecnai 12 (Eindhoven, Netherlands) at 80 KV and photographed by a Mega view G2 camera (Olympus, Japan).

For immunofluorescence analysis, nerves and DRGs were fixed by immersion for 1 h in 4% paraformaldehyde in 0.1 M PBS (1X PBS, pH 7.4), followed by three 10 min washes in 1X PBS. Nerves were then subjected to a sucrose gradient (10%, 20% and 30% sucrose in 1X PBS) and included in optimal cutting temperature compound (OCT, Sakura Finetek) and fast frozen in liquid nitrogen. Tissue was transversally sectioned (10 µm thickness) using a cryostat (Leica, Nussloch, Germany) and mounted on Superfrost Plus slides (Thermo Fisher Scientific). Sections were blocked/permeabilized with 0.1% Triton X-100 and 2% fish skin gelatin (Sigma-Aldrich)

in 1X PBS for 1 h at room temperature (RT) and incubated with primary antibodies in the same solution overnight at 4°C. After 3x 10 min washes with 1X PBS, nerves were incubated in secondary antibodies for 2 h at RT, the washed with 1X PBS and mounted in Fluoromont-G (Electron Microscopy Sciences) with 0.75% DAPI as previously described (Valenzuela et al, 2012). Sections were immunostained using the following antibodies: chicken anti-neurofilament medium chain (NF-M) 1:1000 (#AB5753, Millipore Bioscience Research Reagents), rabbit anti-myelin basic protein (MBP) 1:500 (M3821, Sigma) and rat anti-Cd11b 1:500 (MCA74G, Serotec). Images of tissue sectioning were obtained in an inverted Olympus IX71 fluorescent microscope equipped with a 40X objective (Olympus LUCPlanFLN NA 0.60 Ph2, Olympus, Japan).

For quantifications, at least 3 images were captured per sciatic nerve. Then, a mean value of each parameter to evaluate was obtained of these 3 pictures, and finally it was averaged with the mean value of the animals in each condition. A representative image is shown in every figure. All images were analyzed using Image-J software (NIH, Bethesda, MD, USA).

For electron microscopy analysis, quantifications of semi-thin slides were made by parameters of morphology to identify intact fibers and remyelinated axons by size, axoplasm content, and condensed myelin. Degenerated myelins were identified by decompacted myelin and aberrant compaction of myelin morphology (Fig 4).

6.7 Statistical analysis

Data are shown as mean \pm SEM. Statistical analysis were performed using two-way ANOVA, followed by a Bonferroni post test and Student's t-test and analyzed using GraphPad Prim 5 software.

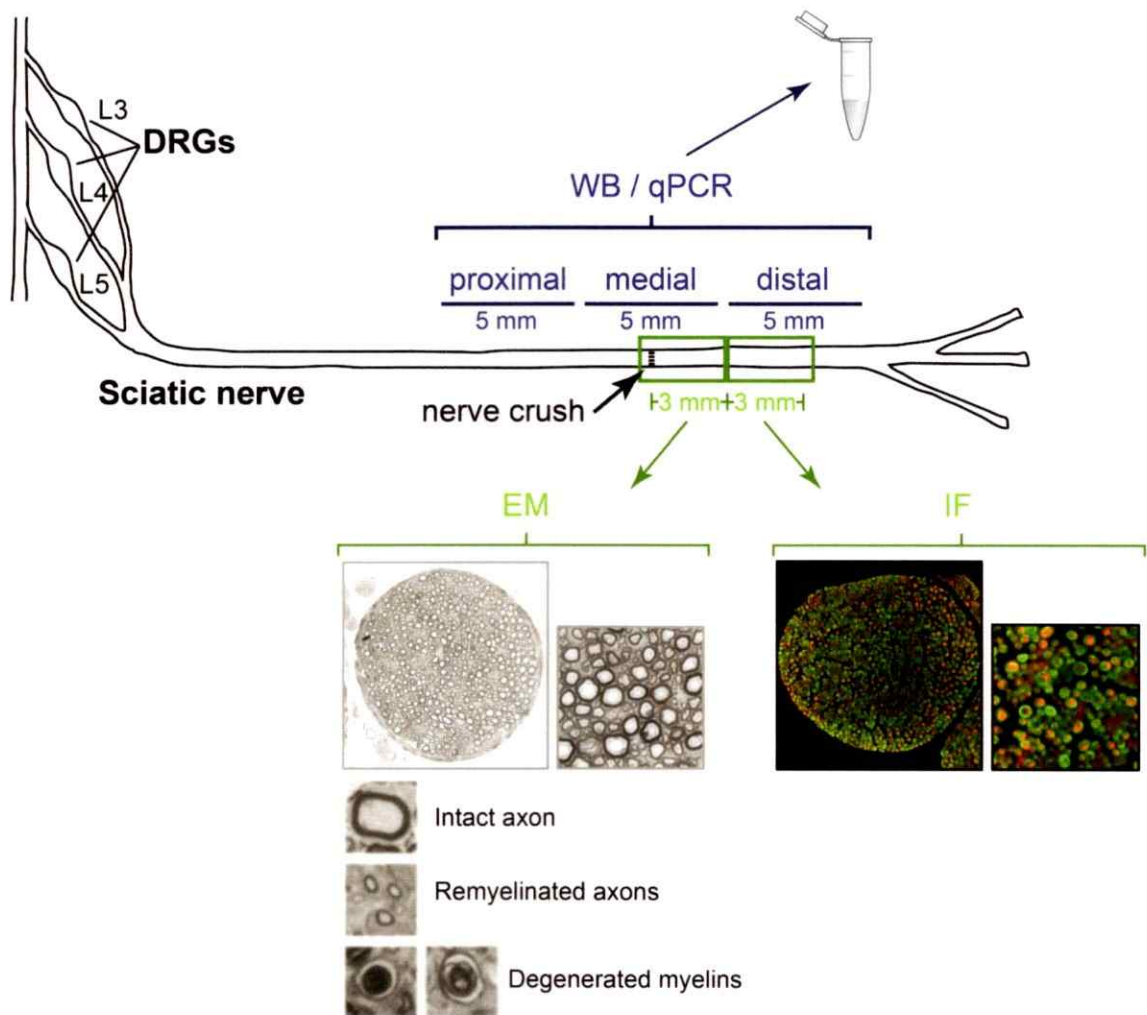


Figure 4. Experimental designs. Sciatic nerves were crushed and at different times post injury a 5 mm section of tissue was extracted in the injury region (medial, M) and adjacent proximal (P) and distal (D) regions for biochemical analysis of protein and mRNA (blue). For histological analysis sciatic nerves were removed at 11 and 14 dpi. A 3 mm region located 3 mm distal to crush site was removed for electron microscopy, the contiguous 3-mm region located 6 mm distal to injury was removed for immunofluorescence analysis (green). To quantify EM parameters we determine criteria for intact axons in uninjured conditions and for remyelinated axons and degenerated myelins in injured nerves. Contralateral nerve was used as uninjured sham control.

7. Results

7.1 Sciatic nerve injury triggers a local upregulation of selective UPR responses.

In order to define the activation of the UPR in the peripheral nervous system, we analyzed the expression of the ER stress-responsive chaperones in the sciatic nerve. To assess the dynamic range of the system to respond to ER stress, wild-type (WT) animals were intraperitoneally injected with tunicamycin (Tm), which inhibits protein *N*-glycosylation and leads to accumulation of proteins in the ER, causing stress (Kozutsumi et al, 1988). After 16 h of Tm injection, the protein level of the chaperones BiP and ERp57 were monitored in the sciatic nerve, liver and brain cortex (Dioufa et al, 2012; Zhang & Kaufman, 2008). We observed an increase in the expression of ER chaperones in all tissues analyzed compared to control conditions. Specifically, Tm induced an increase of 1.52 and 1.38 fold in BiP and ERp57 expression in the sciatic nerve, respectively (Supplementary Fig S1), suggesting that the UPR can be pharmacologically induced in the peripheral nerve.

Then, to characterize the temporal activation of the UPR after sciatic nerve crush, we performed a kinetic analysis and monitored the expression of ER chaperones in sciatic nerve segments containing the crushed region (medial, M), a proximal (P) and distal (D) fragment to the injured zone (Fig 4). After sciatic nerve crush, a progressive increase in BiP and ERp57 levels was detected at early time points, at 12 hours post-injury (hpi) in the medial region compared to contralateral (C) uninjured nerves (Fig 5A and Supplementary Fig S2A) and more markedly at 24 hpi (Fig 5B and Supplementary Fig S2B). At 8 days post-injury (dpi), we detected a peak of BiP expression in the distal

region compared to uninjured nerves (Fig 5C), which corresponds to the nerve region (D) and time (8 dpi) in which axonal regeneration is taking place (Fawcett & Keynes, 1990). Finally, at 21 dpi, when Wallerian degeneration is complete and remyelination of new fibers is underway, BiP protein levels return to basal levels similar to the uninjured condition (Fig 5D).

We also monitored the activation of the ER stress sensor IRE1 α , assessed by the quantification of XBP1 mRNA splicing. Kinetic analysis using real time PCR from samples of the distal region at 2, 8 and 14 dpi revealed a significant increase in XBP1 mRNA splicing at 14 dpi (Fig 5E). This result was then corroborated using another XBP1 mRNA processing assay based in the PstI digestion of a RT-PCR reaction, which resolves both the spliced (XBP1s) and unspliced (XBP1u) forms (Fig 5F). In agreement with the previous results, we observed a significant upregulation of the UPR-target genes *Wfs1* and *Aff3* at 14 dpi (Fig 5G). In contrast, analysis of downstream markers of the PERK pathway revealed no induction in the mRNA levels of the proapoptotic ATF4 effectors *Chop* and *Gadd34* at 2 and 14 dpi (Supplementary Fig S2C and Fig 5H). In summary, our results support the occurrence of an ER stress reaction that specifically engages the IRE1 α /XBP1 axis upon sciatic nerve injury.

We next evaluated locomotor behavior of WT mice in order to characterize functional locomotor recovery using the SFI (for details see Material and Methods, section 6.5) after unilateral sciatic nerve crush. In the control condition (uninjured, day 0), animals have a locomotor index around 0, represented by a normal footprint in the uninjured condition (Fig 6A, uninjured), which change to a negative value near -120, 24 hours after injury determined by an increase in the length (PL parameter) of the paw footprint and a decrease in the width (TS parameter) of the injured limb (Fig. 6A, day 1).

As locomotor recovery proceeds, SFI index returned to value near 0 and footprints are restored to basal conditions at day 21 (Fig 6A and B, day 21). This process is characterized by a reestablishment of the paw prints and has been shown to be partially associated to axonal regeneration. In summary, we were able to characterize a locomotor recovery response after injury as regeneration proceeds, allowing us to determine a possible functional association between UPR activation and a regenerative process.

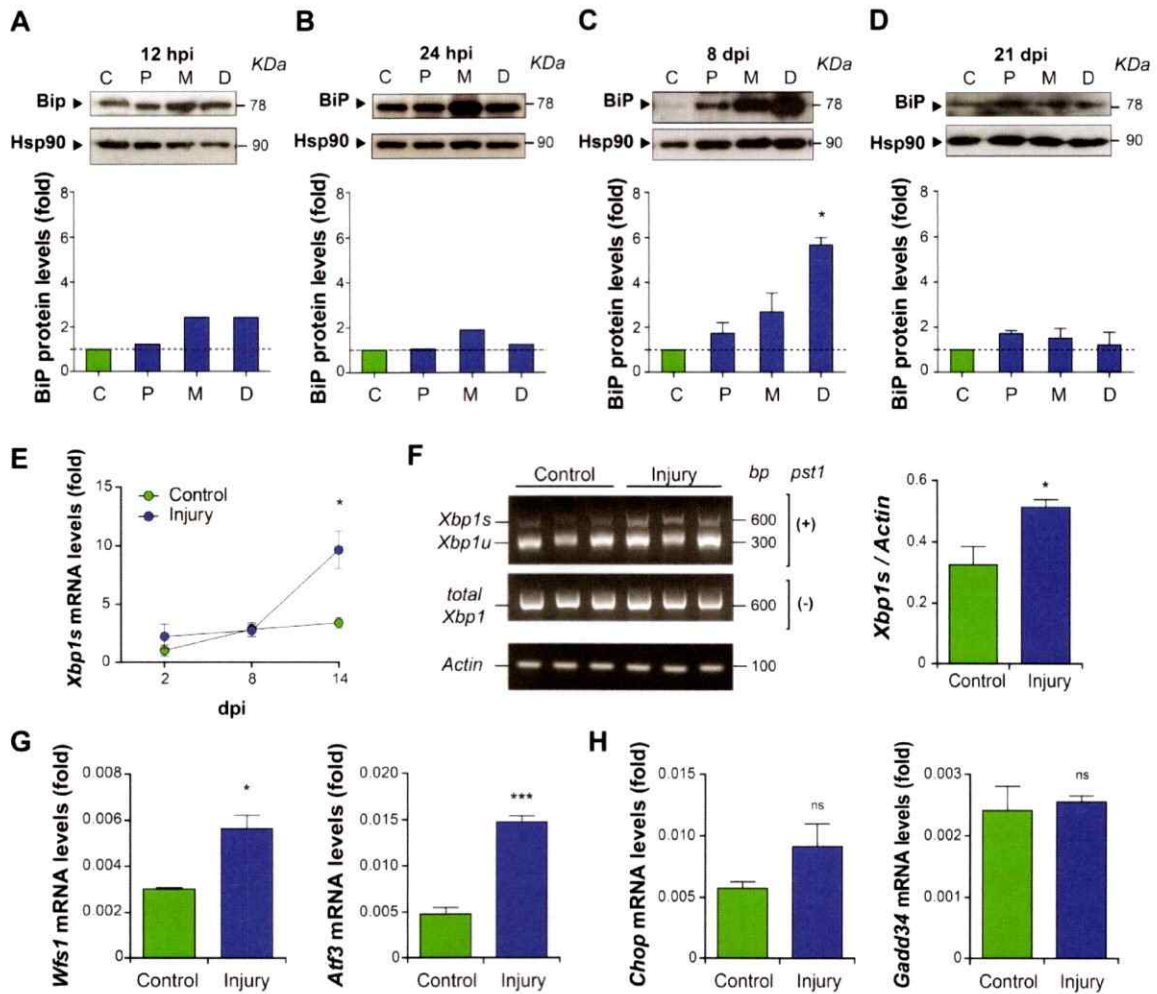


Figure 5. Unfolded protein response is activated after sciatic nerve injury. WT mice were injured and at different days post-injury (dpi) a 5 mm region of the sciatic nerve was removed in the injured region (medial, M) and adjacent proximal (P) and distal (D) for posterior analysis. BiP protein levels were evaluated at (A-B) 12 and 24 hours post injury (hpi) and at (C-D) 8 and 21 days post injury (dpi) in P, M and D regions and compared to contralateral uninjured nerves (label as C). Protein levels were quantified by densitometry and normalized with Hsp90 expression (bottom panel). (E) *Xbp1s* mRNA expression was quantified by real-time PCR in the D region at 2, 8 and 14 dpi. (F) *Xbp1* spliced (*Xbp1s*) and unspliced (*XBP1u*) forms mRNA levels were analyzed in D region at 14 dpi by RT-PCR followed by *PstI* digestion. *Actin* levels were measured as loading control. (G) *Wfs1*, *Atf3*, (H) *Chop* and *Gadd34*, expression was analyzed from sciatic nerves by real-time PCR in uninjured conditions and at 14 dpi in D regions. For panels C to H, data is expressed as mean \pm S.E.M.; * $p < 0.05$, *** $p < 0.001$. Statistical differences were analyzed using student's t-test; $n = 3$ animals per group.

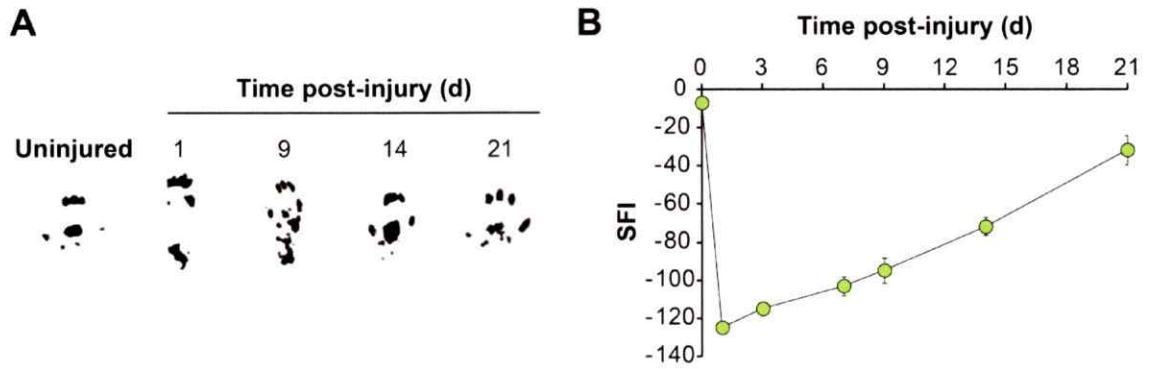


Figure 6. Locomotor recovery in wild-type mice after sciatic nerve injury. **A)** WT animals were injured in the right sciatic nerve and sham operated in the left sciatic nerve. Locomotor recovery was evaluated using the SFI analysis before (0 day) and until 21 days after nerve injury. **B)** Representative footprints of the damaged hindlimb at different times post-injury. Data are shown as mean \pm S.E.M.; $n = 7$ animals.

7.2 XBP1 deficiency decreases locomotor recovery, myelin removal and axonal regeneration after sciatic nerve injury.

To evaluate the relevance of the UPR to locomotor recovery and tissular changes associated to nerve damage, we performed genetic manipulation of two key UPR transcription factors in mice. First, we investigated the functional contribution of XBP1 to axonal degeneration and regeneration using the Nestin-Cre LoxP system to specifically ablate XBP1 expression in the nervous system (XBP1^{Nes-/-}) using a mouse model we have previously characterized (Hetz et al, 2008). We confirmed the expression of Cre and the deletion of exon II of the *Xbp1* gene in the dorsal root ganglia (DRG) and sciatic nerve, in addition to cerebellum (positive control; Supplementary Fig S3A and S3B), suggesting the *xbp1* deficiency in neurons and Schwann cells, principally. After sciatic nerve crush, locomotor function was estimated using the sciatic nerve functional index (SFI, Inserra et al, 1998). Analysis of this behavioral test over time indicated a delay in locomotor recovery after nerve crush in XBP1^{Nes-/-} mice compared to XBP1^{WT} littermate control animals (Fig 7A). The differences in locomotor capacity between genotypes were significant as a group and at intermediate stages of recovery, but in both strains a complete recovery was reached at 21 dpi.

To investigate morphological changes associated to the regeneration process of nerve fibers upon nerve crush, we studied tissue sections by electron microscopy (EM). Since a significant difference in locomotor recovery was found at 14 dpi, we used this time point for EM analysis. In uninjured conditions we observed no differences in the axonal morphology in either myelinating (Fig 7B, white arrowhead) or unmyelinating (Fig 7B, asterisk) fibers and in myelin sheath compaction (Fig 7B, black arrowhead)

between genotypes. At 14 dpi, we noticed an augmented content of degenerated myelins (Fig 7B, black arrows) and decreased number of remyelinated fibers in XBP1^{Nes-/-} compared to XBP1^{WT} control mice (Fig 7B, white arrows). Quantitative analysis of these morphological parameters was then performed in semi-thin nerve cross sections, observing a slight increase in the number of degenerated myelins and a significant reduction in axonal regeneration in XBP1^{Nes-/-} mice compared to control animals (Fig 7C). Together these results suggest that XBP1 expression modulates the axonal regenerative process and locomotor recovery after sciatic nerve crush.

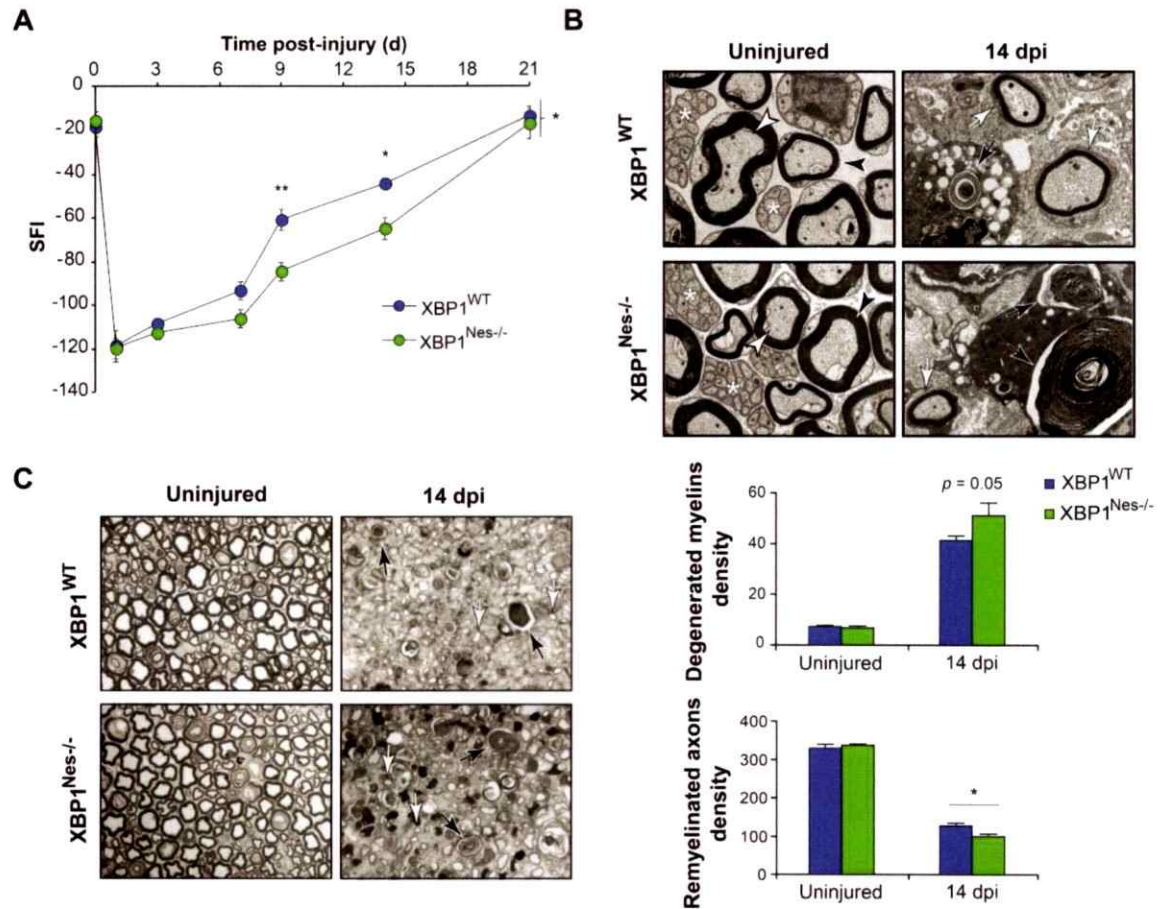


Figure 7. XBP1 deficiency decreases myelin removal, axonal regeneration and locomotor recovery after sciatic nerve injury. (A) XBP1^{WT} and XBP1^{Nes-/-} mice were crush injured in the right sciatic nerve and sham operated in the left sciatic nerve. Locomotor recovery was evaluated using the SFI analysis before (0 day) and at indicated time points. (B) Electron microscopy of uninjured and distal regions of 14 days injured sciatic nerves from XBP1^{WT} and XBP1^{Nes-/-} mice. White arrowheads indicate intact myelinated axons, black arrowheads, intact myelins and asterisks indicate unmyelinated axons. Black arrows point to degenerated myelins and white arrows, to remyelinated axons. (C) Transversal semi-thin sections of sciatic nerves stained with toluidine blue from uninjured and at 14 dpi XBP1^{WT} and XBP1^{Nes-/-} mice. Sections were obtained 3 mm distal to crush region. Black and white arrows indicate demyelinated and regenerated fibers, respectively (left panel). Quantification of degenerated myelins and remyelinated fibers density is presented (right panel). Data are shown as mean \pm S.E.M.; *, $p < 0.05$; **, $p < 0.01$. SFI data were analyzed by a two-way ANOVA followed by Bonferroni post test; $n = 7$ animals per group. Morphological data was analyzed at each time point by student's t-test; $n = 3$ animals per group.

7.3 Ablation of ATF4 does not affect Wallerian degeneration and locomotor recovery after nerve injury.

To define if the effects of XBP1 were specific to this UPR signaling branch, we next assessed the contribution of ATF4 to locomotor recovery after nerve damage. To this end, ATF4 full knockout (ATF4^{-/-}) mice (Masuoka & Townes, 2002) were subjected to a sciatic nerve crush and locomotor recovery was monitored using the SFI. Surprisingly, despite previous *in vitro* observation suggesting a proapoptotic role of this pathway in Schwann cells (Mantuano et al, 2011), the locomotor recovery of ATF4^{-/-} and control wild-type animals was virtually identical at all time points, reaching full recovery at 21 dpi (Fig 8A). Evaluation of morphological parameters by EM revealed no basal differences in the nerve ultrastructure between genotypes in uninjured conditions. Also, EM analysis in the distal stump of crushed sciatic nerves at 14 dpi showed no changes in the clearance of degenerated myelins and remyelination of regenerated axons between ATF4^{-/-} and control mice as measured using quantitative morphometric analysis (Fig 8B and C). These results are consistent with the small induction of ATF4 target genes (Fig 5H), suggesting that the XBP1-UPR branch is specifically activated after nerve injury, impacting axonal regeneration and locomotor recovery after peripheral nerve damage.

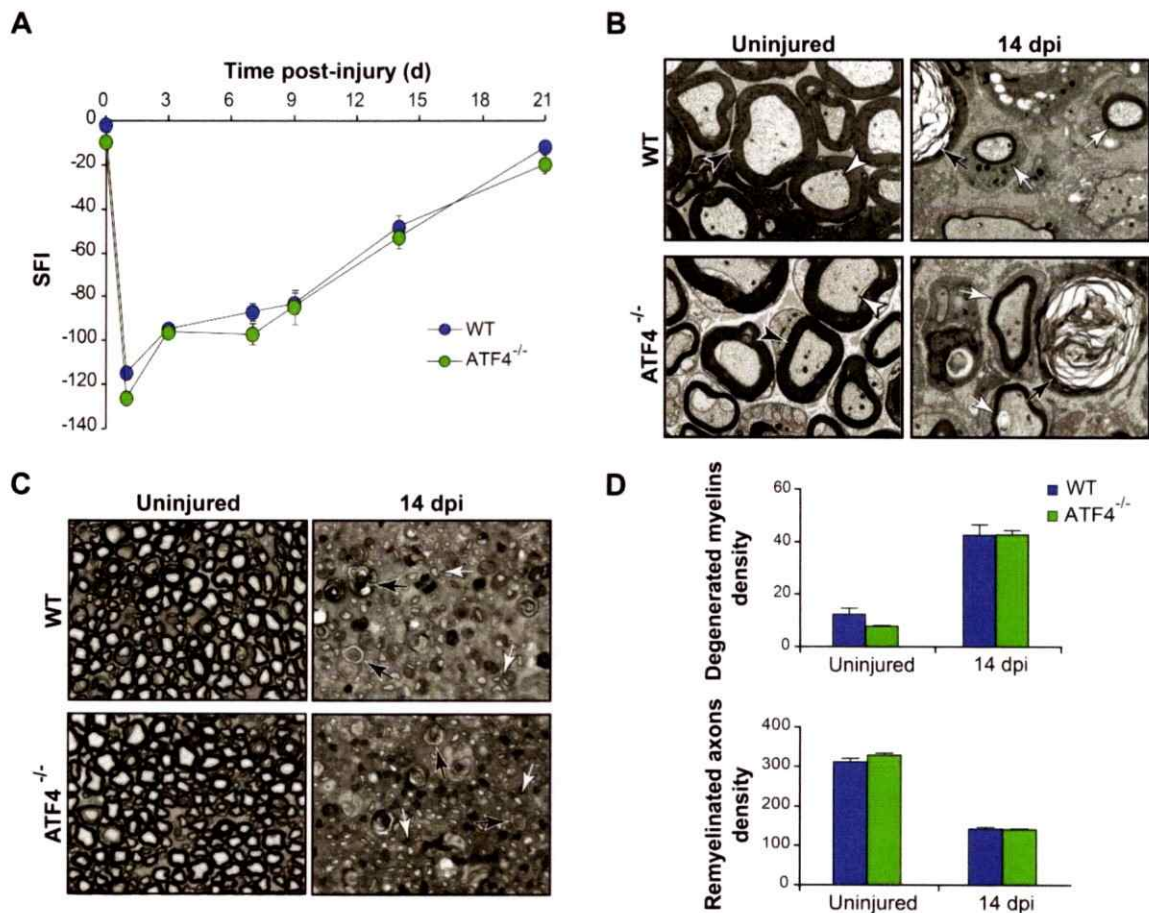


Figure 8. ATF4 deficiency does not affect Wallerian degeneration after peripheral nerve injury. (A) ATF4^{-/-} and WT mice were injured in the right sciatic nerve and sham operated in the left sciatic nerve. Functional recovery of the damaged hindlimb was estimated using the SFI over time. (B) Electron microscopy of sciatic nerves from WT and ATF4^{-/-} mice in uninjured conditions and at 14 dpi. In uninjured conditions white arrowheads point intact myelinated axons and black arrowheads, intact myelins. At 14 dpi, black arrows indicate degenerated myelins and white arrows, remyelinated axons. (C) Toluidine blue-stained transversal semithin sections in control-uninjured nerves and at 14 dpi from WT and ATF4^{-/-} mice. Black arrows points degenerated myelins and white arrows, remyelinated axons. Measurement of degenerated myelins and remyelinated fibers density is presented from transverse semi-thin sections from each mouse strain (right panel). Data is shown as mean ± S.E.M.; SFI data were analyzed by a two-way ANOVA followed by Bonferroni post test; n = 7 animals per group. Morphological data were analyzed by student's t-test at each time point; n = 3 animals per group.

7.4 Overexpression of XBP1s in the nervous system accelerates myelin removal, axonal regeneration and locomotor recovery after nerve injury.

We then generated a genetic strategy to pre-adapt the proteostasis network and reduce ER stress levels in the nerve by forcing UPR-transcriptional responses in neurons and Schwann cells and then test the consequences on Wallerian degeneration and axonal regeneration. To this end, we generated a mouse model that overexpresses spliced XBP1 under the control of the prion promoter (Tg^{XBP1s}) in the nervous system. These animals are viable and born on a mendelian rate, and did not show any spontaneous motor phenotype. We confirmed the overexpression of XBP1s in DRGs, cerebellum and sciatic nerve using real time PCR (Supplementary Fig S3C). We first evaluated locomotor recovery after nerve crush in Tg^{XBP1s} and non-transgenic littermates (Non-Tg). Remarkably, SFI analysis revealed that Tg^{XBP1s} mice have a significant increase in locomotor recovery at 9 and 14 days after nerve crush compared to littermate control mice (Fig 9A). Consistent with these results, Tg^{XBP1s} nerves exhibited a reduction in the content of degenerated myelins and increased number of remyelinated axons compared to control sciatic nerves at 14 dpi (Fig 9B and C). Similar results were obtained when axonal and myelin morphology was analyzed at 11 dpi (Supplementary Fig S4). These results suggest that artificial enforcement of XBP1s increases the regenerative capabilities of injured peripheral nerves.

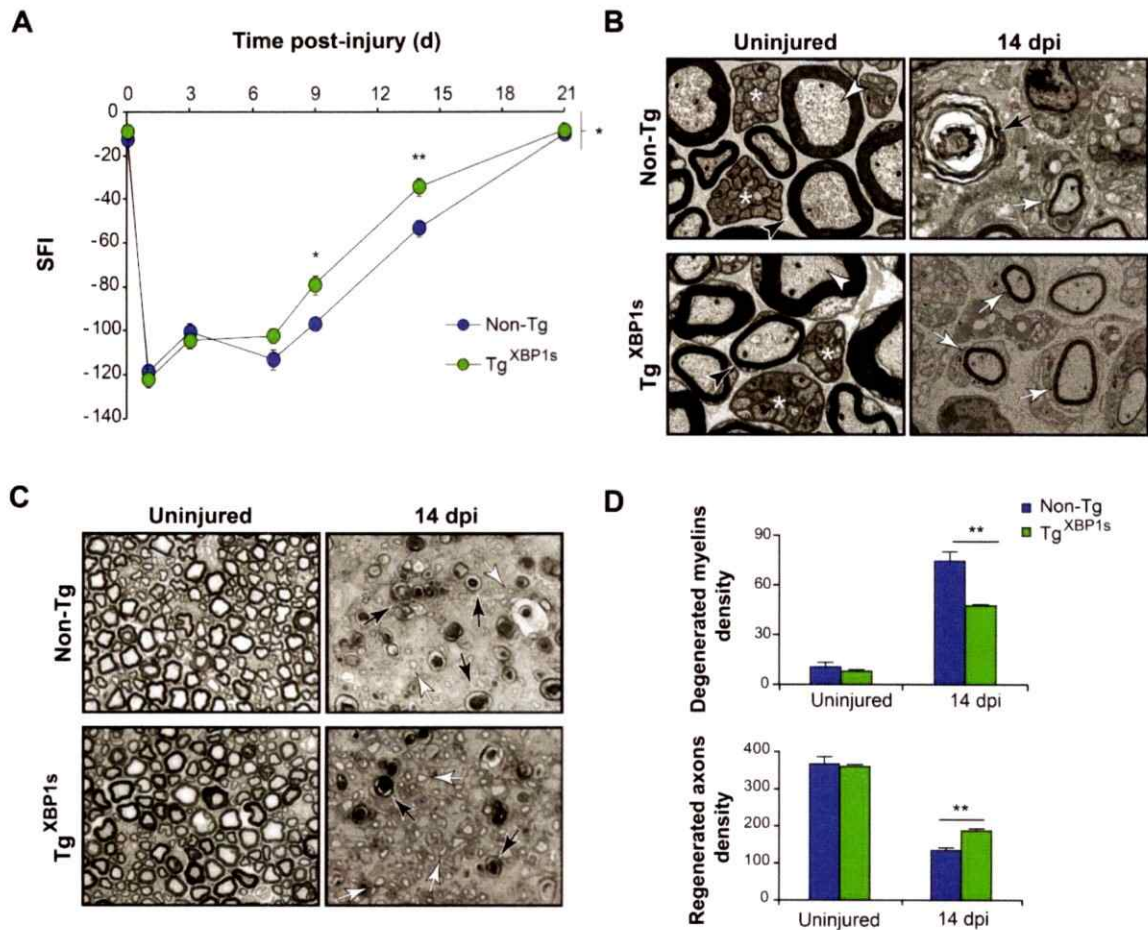


Figure 9. Overexpression of XBP1s increases myelin removal, axonal regeneration and locomotor recovery after peripheral nerve injury. (A) Tg^{XBP1s} and Non-Tg mice were damaged in the right sciatic nerve and sham operated in the left sciatic nerve. Locomotor performance was evaluated using the SFI analysis before (0 day) and at the indicated time points. (B) Uninjured and distal regions of 14 days injured sciatic nerves from Tg^{XBP1s} and Non-Tg mice were analyzed by electron microscopy. In control conditions black arrowheads indicate compact myelin, white arrowheads, myelinated axons and asterisk, unmyelinated axons. At 14 dpi, white and black arrows point remyelinated fibers and degenerated myelins, respectively. (C) Tg^{XBP1s} and Non-Tg sciatic nerves from uninjured and at 14 dpi. Transversal semi-thin sections were obtained 3 mm distal to the crush region and stained with toluidine blue. Quantification of the number of degenerated myelins and remyelinated fibers was performed per area from transverse semi-thin sections of each mouse strain (right panel). Data are shown as mean \pm S.E.M.; *, $p < 0.05$; **, $p < 0.01$. SFI data were analyzed by a two-way ANOVA followed by Bonferroni post test; $n = 7$ animals per group. Morphological data were analyzed by student's t-test at each time point; $n = 3$ animals per group.

7.5 XBP1 modulates macrophage infiltration after sciatic nerve injury.

Removal of myelin debris after nerve damage is mediated early on by Schwann cells and later by macrophages that are recruited to the injured region (Hirata & Kawabuchi, 2002), contributing to axonal regeneration by eliminating inhibitory factors associated to myelin debris (Stoll et al, 2002). We therefore evaluated the impact of XBP1 to the recruitment of Cd11b-positive (Cd11b⁺) macrophages in damaged peripheral nerves from animals with manipulated levels of XBP1. A low density of macrophages was observed in both XBP1^{Nes^{-/-}} and wild-type animals in uninjured conditions (Fig 10A, upper panel). A significant increase in the density of Cd11b⁺ macrophages was observed in XBP1^{WT} but not in XBP1^{Nes^{-/-}} mice at 14 dpi (Fig 10A and B). Importantly, in XBP1^{Nes^{-/-}} mice macrophage density after injury was comparable to the density measured in uninjured conditions (Fig 10A and B). We then analyzed the extent of macrophage infiltration in Tg^{XBP1s} mice. Consistent with our previous results, analysis of Tg^{XBP1s} mice revealed a significant enhancement in macrophage recruitment compared to Non-Tg littermate control animals at 14 dpi (Fig 11A and B). Of note, the extent of macrophage infiltration observed in the controls of both groups after nerve crush was different, probably reflecting slight changes in genetic background of both mice strains. Thus, XBP1 expression in the nervous system improves pro-regenerative process that may directly or indirectly result in improved macrophage recruitment to the damaged nerve.

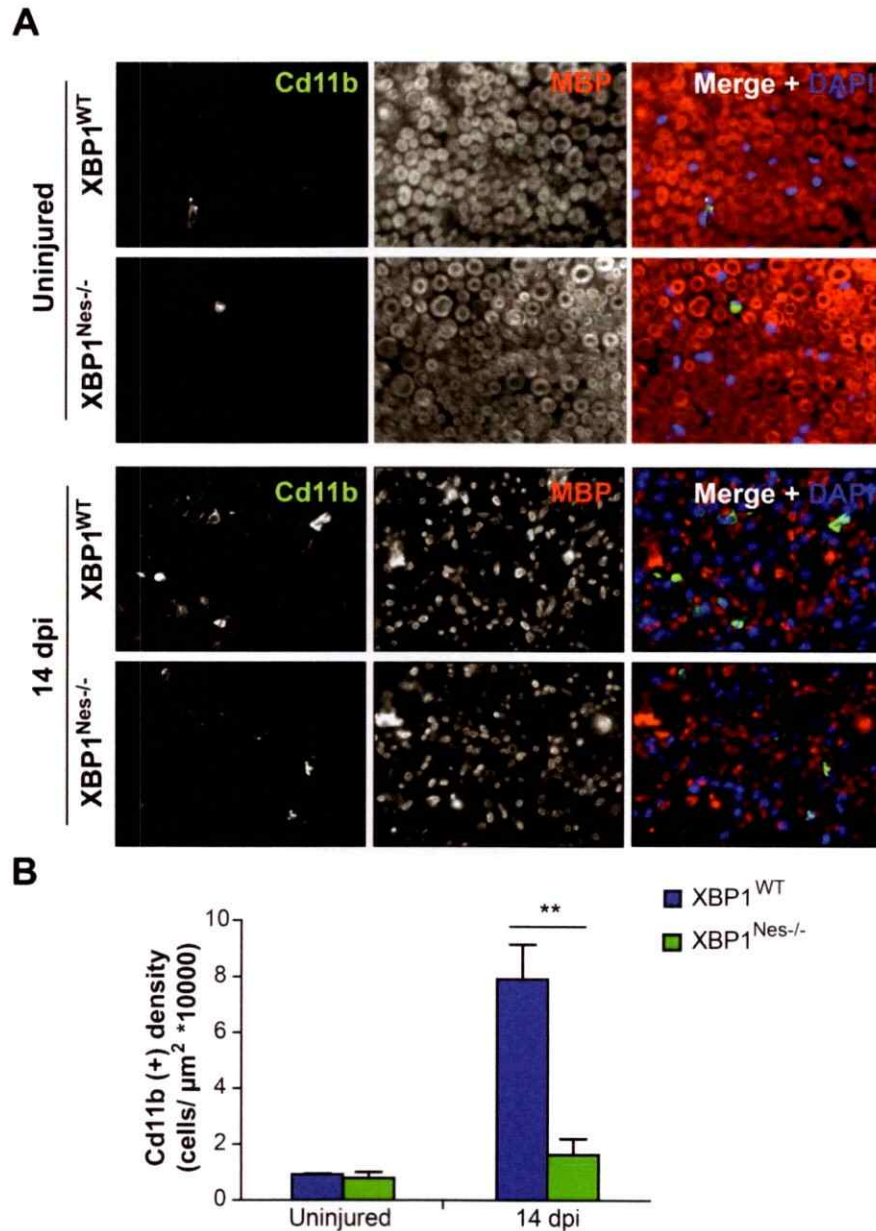


Figure 10. XBP1 deficiency decreases macrophage infiltration after sciatic nerve injury. (A) XBP1^{Nes-/-} and control XBP1^{WT} nerves were processed by immunofluorescence in uninjured conditions (upper panel) and 14 dpi (lower panel). Sciatic nerves were analyzed for Cd11b (green) to stain macrophages (left panel) and MBP (red) to evaluate the myelin sheath (center panel). Nuclei were stained with DAPI (blue). (B) The density for Cd11b+ staining was quantified 14 days after injury in XBP1^{Nes-/-} and XBP1^{WT} mice. Data are expressed as mean ± S.E.M. ** $p < 0.01$. Student's t-test; $n = 3$ animals per group.

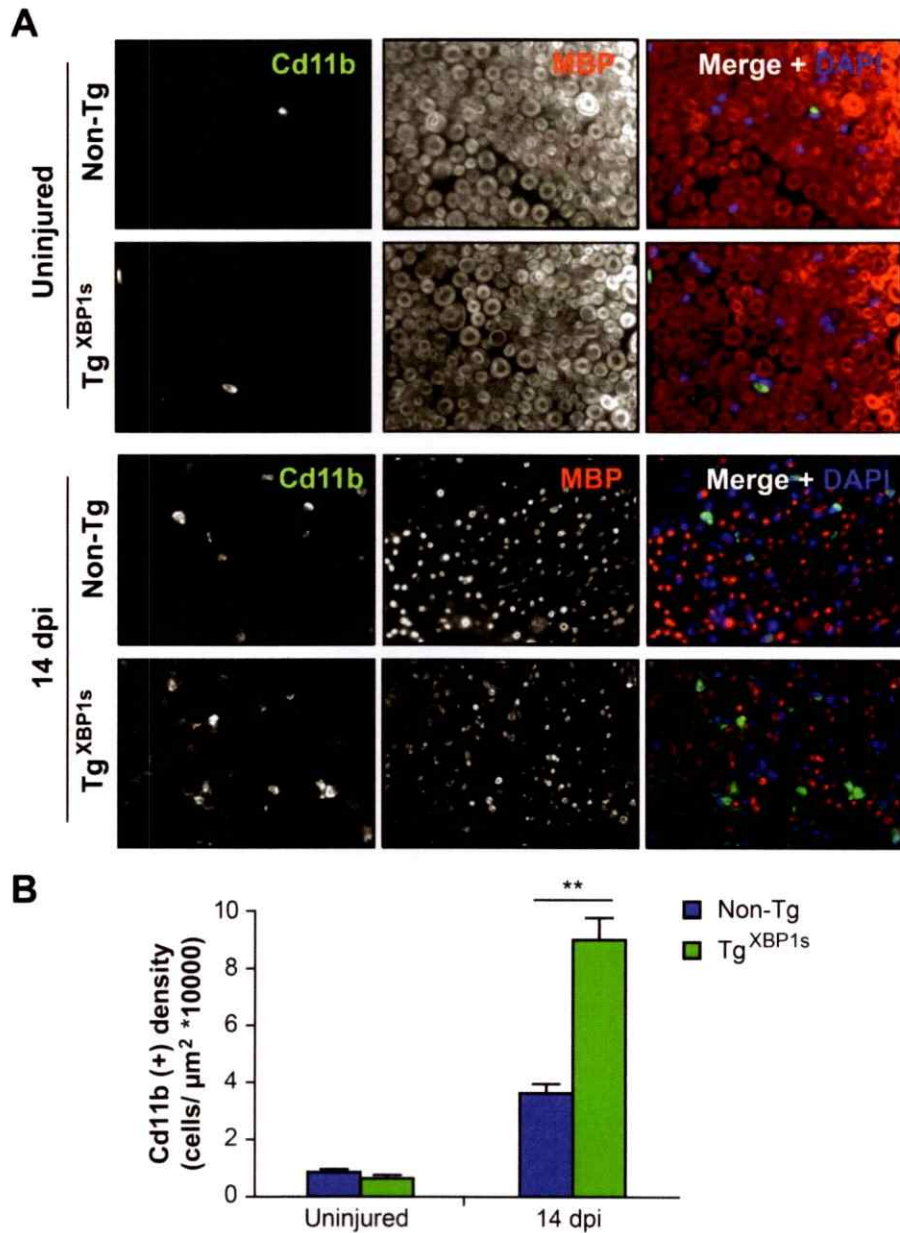


Figure 11. Overexpression of XBP1s increases recruitment of macrophages after injury. (A) Tg^{XBP1s} and Non-Tg sciatic nerves were processed by immunofluorescence for Cd11b (green) to immunolabel macrophages (left panel), MBP (red) to evaluate the myelin sheath (center panel), and DAPI to stain nuclei (blue) in uninjured conditions (upper panel) and at 14 dpi (lower panel). (B) The density for Cd11b+ cells was quantified 14 days after injury in Tg^{XBP1s} and Non-Tg mice. Data are expressed as mean \pm S.E.M. ** $p < 0.01$. Student's t-test; $n = 3$ animals per group.

7.6 Local XBP1s gene transfer to DRGs enhances axonal regeneration after peripheral nerve damage.

Our previous results are indicative of a functional role of XBP1 in the regenerative response observed in the PNS after nerve injury. Since both mouse models used to perform XBP1 gain- and loss-of-function target neurons and possibly other cell types, including glial cells, and the genetic manipulation is active since embryonic development, we next evaluated the consequences of delivering an active form of XBP1 selectively to neurons of adult animals to assess a possible cell-autonomous contribution of XBP1 to axonal regeneration. We developed a neuronal serotype 2 Adeno-Associated Viruses (AAV) to overexpress XBP1s specifically in sensory neurons in addition to green fluorescent protein (EGFP) to identify transduced axons as we recently reported (Valenzuela et al, 2012; Valdés et al, 2014). We then injected DRGs with AAVs to deliver XBP1s (AAV XBP1s/EGFP) or EGFP alone (AAV EGFP) in 2 month-old mice. Injections were performed in DRGs from lumbar vertebrae 3 (L3) and 4 (L4) as the neurons located in these DRGs project their axons to the sciatic nerve (Fig 12A). The efficiency of viral transduction was confirmed by inspection of EGFP signal 7 days after AAV injection, observing that both neuronal somas at DRGs and axons in the sciatic nerve were positive for EGFP (Fig 12B and C).

Then, the sciatic nerve was crushed and regenerated EGFP-positive axons were quantified in the distal nerve stump at 14 dpi. Axonal regeneration was evaluated by quantifying the number of EGFP-positive axons co-labeled with the axonal marker neurofilament medium chain (NF-M) in cross sections at 3 mm distal to the crush region (Fig 12D). Regenerated axons were normalized to the number of EGFP- and NF-M-

positive axons at 6 mm proximal to the crush region of the same nerve, to control for possible differences in AAV-transduction efficiency between animals. Remarkably, we observed a significant 1.5 fold increase in the number of double-positive regenerated axons when XBP1s was expressed in comparison to control axons expressing EGFP alone (Fig 12E). These results suggest that forced expression of active XBP1s in sensory neurons can enhance the intrinsic regenerative capabilities of neurons after peripheral nerve damage.

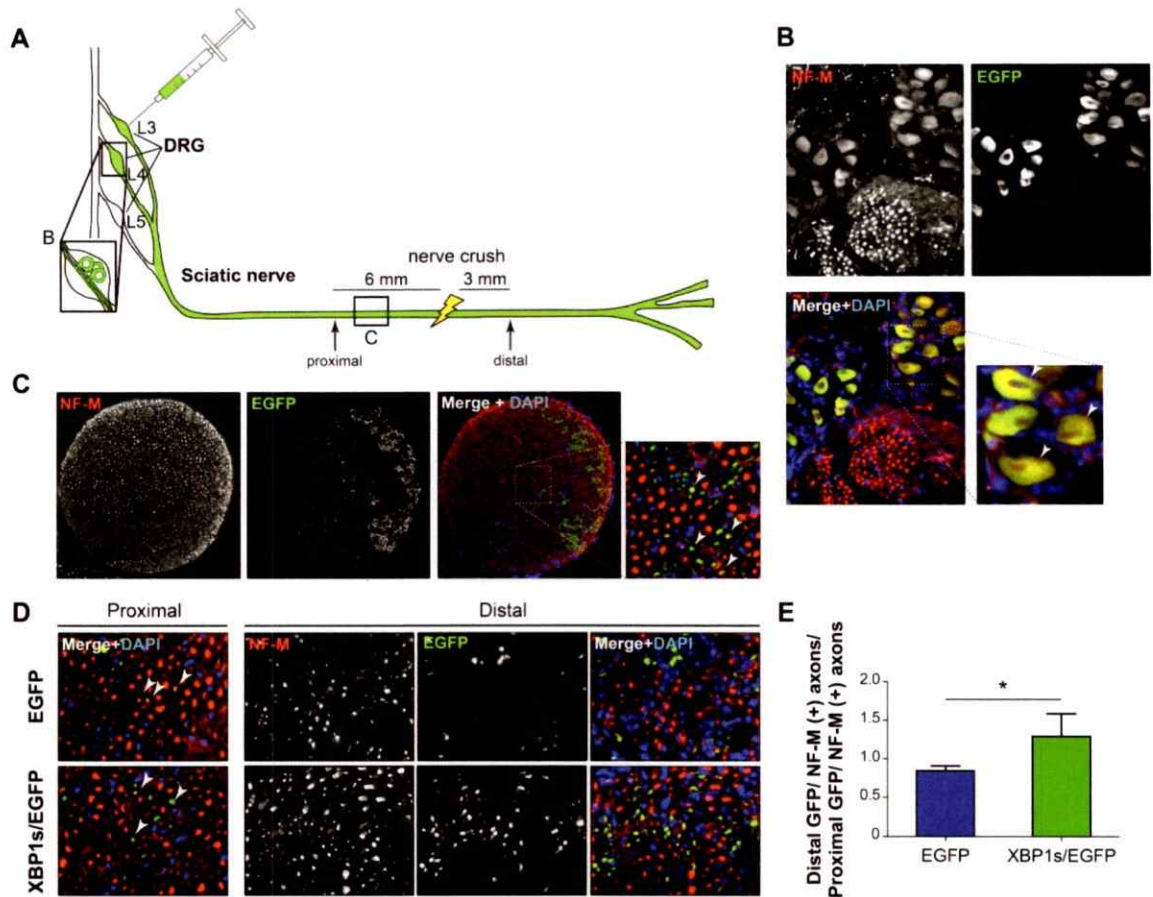


Figure 12. XBP1s overexpression in neurons enhances axonal regeneration *in vivo*. (A) Schematic representation of the experimental design. WT mice were injected with 1 μ l of AAV EGFP or AAV XBP1s/EGFP in L3 and L4 DRGs. EGFP expression was used to identify transduced neurons. At 7 days post injection the sciatic nerve was crushed at the sciatic notch level (yellow light bolt) and at 14 dpi the nerves were dissected and analyzed in transverse sections 3 mm distal to the injury (black arrow, distal) and normalized to EGFP-positive axons proximal to the crush (black arrow, proximal). (B) EGFP expression of infected neurons from DRGs (B box), 7 days after injection in uninjured nerves. NF-M immunostaining was used to identify neuronal somas and axons. (C) Cross section of an uninjured nerve 7 days after AAV injection (C box). EGFP fluorescence in green, immunostained for NF-M (red) and counterstained using DAPI (blue). Transduced somas and axons are indicated with white arrowheads in the insets of B and C. (D) Axonal regeneration in the sciatic nerve was evaluated in AAV EGFP (upper panel) and AAV XBP1/EGFP (lower panel) injected DRGs at 14 dpi (E) Quantification of mean EGFP+/NF-M+ axons in distal region normalized to proximal EGFP+/NF-M+ axons of the same sciatic nerve from AAV EGFP and AAV XBP1s/EGFP injected mice. Data are expressed as mean \pm S.E.M.; *, $p < 0.05$. Student's t-test was performed for statistical analysis; $n = 3$ per condition.

8. Discussion

Alteration to the proteostasis network is emerging as a relevant player in most common neurodegenerative diseases involving protein misfolding (Hetz & Mollereau, 2014). Although extensive reports are available describing the impact of the UPR to neuronal degeneration, no studies have determined the functional impact of ER stress to peripheral axonal degeneration and regeneration.

Recent correlative studies have associated an early activation of ER stress and UPR markers, specifically in the neuronal cell body and in Schwann cells, as well after different models of peripheral nerve injury (Saxena et al, 2009; Mantuano et al, 2011; Penas et al, 2011). Since the UPR has dual roles in both cell survival and cell death, the impact of this pathway to peripheral nerve injury has remains undefined. In this study, we confirmed a progressive and local activation of the UPR after sciatic nerve damage. Importantly, we demonstrated for the first time a functional and selective role of the IRE1 α /XBP1 pathway in locomotor recovery and axonal regeneration after sciatic nerve injury using gain- and loss-of-function approaches.

In addition, an increase in the expression of ER chaperones, specifically BiP, was observed in the injury region at early stages and in distal region at later stages, where axonal degeneration and regeneration takes place, indicating the possibility of a propagating stress signal which would initiate in the injury region and then spreads to distal axonal domains as degeneration proceeds, activating a stress response in Schwann cells along the tissue, as it has been proposed previously (review in Taylor et al, 2013) for tumor cell lines (Mahadevan et al, 2011; Mahadevan et al, 2012) and in systemic conditions in *C. elegans* (Richardson et al, 2010; Taylor & Dillin, 2013).

Using genetic manipulation of specific key UPR components, we demonstrated for the first time a functional role of this pathway in locomotor recovery and axonal regeneration after sciatic nerve injury. A delay in locomotor recovery was observed in XBP1^{Nes-/-} mice, associated with a slight decrease in myelin removal and axonal regeneration. Unexpectedly, genetic deletion of *atf4* had no effect in the clearance of myelin debris, extension of regenerating axons or in locomotor recovery in comparison to control animals, demonstrating a differential role of these two UPR pathways. Consistent with these findings, previous evidence revealed that eIF2 α phosphorylation and CHOP expression are repressed in dedifferentiating Schwann cells following nerve injury (Mantuano et al, 2011). We also observed that although XBP1 mRNA splicing was significantly induced after nerve crush, *Chop* and *Gadd34* remained unchanged. In contrast, *in vitro* studies using *Chop* deficient Schwann cells revealed an important proapoptotic activity of this factor upon pro-inflammatory challenges (Mantuano et al, 2011) and in Charcot-Marie-Tooth-1B disease (Pennuto et al, 2008; D'Antonio et al, 2013). Finally, another study indicated that sciatic nerve injury does not activate the PERK signaling branch in motoneurons with injured axons (Penas et al, 2011). Therefore, based on these reports and the comparison presented here using XBP1 and ATF4 deficient animals, we speculate that selective activation of IRE1 α pathway, but not the PERK axis, may operate as an adaptive response allowing successful regeneration and locomotor recovery after neuronal damage.

Accumulating studies in models of neurodegeneration support the idea that the contribution of each UPR signaling branch to the disease process is complex and highly dependent on the disease-triggering mechanisms and the cell type affected (Hetz & Mollereau, 2014). For example, we have shown that targeting either XBP1 or ATF4 in

SCI models actually diminishes locomotor recovery after mechanical damage to the spine, possibly associated to reduced oligodendrocyte survival (Valenzuela et al, 2012). Besides, other reports have shown that expression of CHOP exacerbates tissue damage after SCI (Ohri et al, 2013). In contrast, XBP1 deficiency does not have an effect after optic nerve injury, whereas CHOP expression operates as a relevant proapoptotic factor in retinal neurons (Hu et al, 2012). In ALS, XBP1 or ATF4 deficiency are protective through the control of autophagy or apoptosis, respectively (Hetz et al, 2009; Matus et al, 2013), whereas in Huntington's disease only XBP1 deficiency has beneficial effects (Vidal et al, 2012). In contrast, in prion related disorders, XBP1 is irrelevant (Hetz et al, 2008), whereas PERK has a pro-degenerative activity (Moreno et al, 2012, 2013). Based on these results, we speculate that the distinctive UPR responses triggered in the PNS versus the CNS might help explaining the differential regenerative capabilities of each nervous system compartments.

Remarkably, overexpression of XBP1s in mice produced an enhancement of locomotor recovery after injury, associated to faster myelin degeneration, an increase in axonal regeneration and an enhanced recruitment of macrophages after injury, suggesting a pro-regenerative mechanism associated to IRE1 α /XBP1 signaling. XBP1 expression may have a functional consequence during tissular remodeling activity after injury possibly associated with myelin removal. Interestingly, the importance of the UPR in other tissues also involves activities beyond the control of protein folding, quality control and lipid synthesis, where this pathway modulates cell differentiation and dedifferentiation programs (Cornejo et al, 2013), a phenomena we predict will be relevant also in the context of Schwann cell biology. XBP1 expression is fundamental for the differentiation of many distinct cell types, including B lymphocytes (Zhang et al,

2005; Reimold et al, 2001; Iwakoshi et al, 2003), zymogenic cells in the gastric epithelium (Huh et al, 2010), exocrine pancreas and salivary glands (Lee et al, 2005), among other cell types (Hetz et al, 2011). In chondrocytes, ER stress reprogram the cell towards a dedifferentiation process into non-secreting cells, probably operating as a protective response (Tsang et al, 2007); and a similar concept was recently validated in cancer models (Del Vecchio et al, 2014). Differentiated myelin-forming Schwann cells produce massive amounts of lipids and proteins, with transmembrane proteins trafficking through the ER accounting for near 20-50% of total proteins (Patzig et al, 2011). Based on this fundamental aspect of Schwann cell physiology, it is feasible to propose that this specific cell type may be more prompt to undergo ER stress after sciatic nerve damage. In agreement with this concept, ER stress has been extensively reported to drive oligodendrocyte death in models of multiple sclerosis (Lin & Popko, 2009).

In the same way, ER stress could be mediating adaptive mechanisms related to changes in the differentiation stage of Schwann cells after nerve injury, having a correlative effect on myelin degeneration, secretion of cytokines and chemokines and possibly in the secretion of trophic factors that enhances regeneration, affecting directly the recruitment of macrophages and the extension of regenerated axons. According to this, XBP1 has also a relevant function in the innate immune system, controlling cytokine production in macrophages (Martinon & Glimcher, 2011). Since IL-6 is expressed by dedifferentiated Schwann cells and is involved in macrophage recruitment (Tofaris et al, 2002), the possible contribution of the UPR to the inflammatory microenvironment remains to be determined. Additional experiments in Schwann cells of XBP1^{Nes-/-} or Tg^{XBP1s} mice, including the evaluation of myelinated-associated genes

like P0, MBP or periaxin versus dedifferentiated markers (e.g. p75, krox24), together with the expression of cytokines (LIF, TNF- α , MCP-1 and interleukins) will be required. These experiments will help us to demonstrate the role of the UPR pathway in the local events associated with the progression of the Wallerian degeneration mechanism.

Finally, we tried to differentiate the implications of UPR activation specifically in the different cell types involved in axonal regeneration. We developed a gene therapy approach for XBP1s using AAV treatment. Overexpression of the active form of XBP1 in sensory neurons demonstrated a remarkable increase in axonal regeneration, suggesting that overexpression of the UPR machinery could enhance axonal regeneration in a cell-autonomous manner. Since retrograde injury signals contributes to the transition into a regenerative state (Jung et al, 2012; Rishal & Fainzilber, 2014), local activation of IRE1 α and XBP1 mRNA splicing may provide an axonal-ER signal proximal to the site of nerve injury to engage a regenerative program in the neuronal soma. A similar concept was recently reported for the ATF6 family member LUMAN/CREB3 (Ying et al, 2014). Local cleavage of LUMAN after axonal injury leads to the retrograde transport of the basic leucine zipper transcription factor domain to the nucleus, contributing to axonal regeneration (Ying et al, 2014). Importantly, LUMAN also controls ER stress genes (Liang et al, 2006; DenBoer et al, 2005). Since XBP1s and ATF6 heterodimerizes to control a subset of UPR target genes (Shoulders et al, 2013), and ATF6 can upregulate XBP1 mRNA (Yoshida et al, 2001), it will be interesting to study if both LUMAN and XBP1s cooperatively modulate gene expression programs associated to axonal regeneration. In addition, previous evidence demonstrated that XBP1 promote neurite outgrowth and axonal branching in the presence of the neurotrophic factor BDNF in culture CNS neurons (Hayashi et al,

2007), providing evidence that suggest that in the PNS, overexpression of XBP1 in the presence of injury-induced BDNF release (Zhang et al, 2008; Yao et al, 2013) might enhance axonal regeneration.

Additional experiments including analysis of *xbp1s in vitro* in neurites of DRGs explants by qPCR, specific measure of axonal XBP1s using a novel transgenic mice model (XBP1s-GFP mice) by histochemical analysis and the analysis of the expression of *xbp1s* in DRGs *in vivo* after injury are being developed at the time in the lab to test the idea of a retrograde injury signal in the neuronal-autonomous response.

To determine the specific role of Schwann cells in axonal regeneration, we tried to exclusively transduce glial cells with XBP1s. Nevertheless, technical problems precluded the completion of these experiments, including the AAV serotype used that was directed to infect mainly neurons (AAV2.XBP1s/EGFP). In addition, using *in vivo* electroporation a small fraction of Schwann cells were transduced. However, it will be important to determine the role of UPR activation in Schwann cells and its contribution to the process of axonal regeneration. Possible experiments would include the development of specific AAV with glial serotype, the use of lentivirus particles or to generate a conditional knockout mice for XBP1 using a glial promoter (XBP1^{PD-/-}) to target Schwann cells. This will help defining the specific impact of Schwann cells on myelin removal and axonal growth.

Together, with all these results we proposed that after sciatic nerve damage, ER stress is initiated in the injury region triggering a UPR response, which then spreads this signal to proximal regions through the axon to the neuronal soma, and distal along Schwann cells. Previous evidence, in accordance with our results indicate a differential

activation of the UPR pathways in which the PERK/ATF4 branch is not activated in neurons and Schwann cells after this type of damage, while the IRE1/XBP1 pathway has an important contribution in the local events of Wallerian degeneration, probably related to the dedifferentiation of Schwann cells, secretion of cytokines and chemokines and the recruitment of macrophages, significantly affecting the removal of myelin and axonal debris. In addition, activation of XBP1s in the neuronal soma has a considerable role in the extension of new regenerated fibers, probably related to the regulation of regenerated associated genes, enhancing axonal growth. This, concomitant to the clearance of distal debris and inhibitory factors promote axonal regeneration, and more importantly, functional locomotor recovery, demonstrating for the first time a functional impact of the UPR in Wallerian degeneration. Since new small molecules and gene therapy strategies are available to target the UPR (Hetz et al, 2013), manipulation of the ER proteostasis network might emerge as a new avenue for future therapeutic intervention to improve axonal regeneration.

9. Conclusions

We have demonstrated for the first time the relevance of the UPR in the events of Wallerian degeneration and addressed the impact of this response in axonal regeneration and locomotor recovery after peripheral nerve injury.

We observed that injury to the sciatic nerve triggers an increasing and sustained UPR activation, specifically mediated by the IRE1 α /XBP1 branch. Also, modulation of XBP1 in neurons and glial cells has an effect in the clearance of myelin debris, axonal regeneration and locomotor recovery after damage. We did not observe an effect in ATF4 null animals, corroborating the specific impact of the XBP1 pathway. These results suggest that UPR activation is related to the modulation of the local environment near to the damaged area. Specifically, ER stress may be acting as an adaptive mechanism of Schwann cells response to promote cell dedifferentiation, secretion of trophic factors and cytokines to induce an efficient clearance of myelin and axonal debris, key events for successful regeneration and locomotor recovery.

We also demonstrated that forced overexpression of XBP1s specifically in neurons through gene therapy is sufficient to enhance axonal regeneration, suggesting that the UPR might be also involved in other neuronal changes associated to regeneration, like an early or more sustained expression of regenerating associated genes. Importantly, these results suggest that similar therapies can be used as a therapeutic strategy for peripheral neuropathies and neurodegenerative conditions in the PNS or CNS.

Further experiments are required to describe the precise mechanism of action of the UPR in axonal injury, including the characterization of cytokines profile after injury and the modulation of gene expression of key UPR components to demonstrate a specific role of Schwann cells in this process.

10. References

- Acosta-alvear D, Zhou Y, Blais A, Tsikitis M, Lents N, Arias C, Lennon C, Kluger Y & Dynlacht, B. (2007) XBP1 Controls Diverse Cell Type- and Condition-Specific Transcriptional Regulatory Networks. *Molecular Cell* 27:53–66.
- Allen N & Barres B (2009) Glia — more than just brain glue. *Nature* 457: 675–677.
- Allodi I, Udina E & Navarro X. (2012) Specificity of peripheral nerve regeneration: interactions at the axonal level. *Prog Neurobiol* 98: 16-37.
- Arthur-Farraj P, Latouche M, Wilton D, Quintes S, Chabrol E, Banerjee A, Woodhoo A, Jenkins B, Rahman M, Turmaine M, Wicher G, Mitter R, Greensmith L, Behrens A, Raivich G, Mirsky R & Jessen K (2012) c-Jun reprograms Schwann cells of injured nerves to generate a repair cell essential for regeneration. *Neuron* 75: 633–47.
- Barrette B, Hébert M, Filali M, Lafortune K, Vallieres N, Gowing G, Julien J & Lacroix, S. (2008) Requirement of myeloid cells for axon regeneration. *J Neuroscience* 28: 9363-9367.
- Barrientos S, Martínez N, Yoo S, Jara J, Zamorano S, Hetz C, Twiss J, Alvarez J & Court, F. (2011) Axonal Degeneration Is Mediated by the Mitochondrial Permeability Transition Pore. *The Journal of Neuroscience* 31: 966–978.
- Borchelt D, Davis J, Fischer M, Lee M, Slunt H, Ratovitsky T, Regard J, Copeland N, Jenkins N, Sisodia S & Price D. (1996) A vector for expressing foreign genes in the brains and hearts of transgenic mice. *Genetic analysis: biomolecular engineering* 13: 159-163.
- Brück W. (1997) The role of macrophages in Wallerian degeneration. *Brain Pathol* 7: 741-752.
- Calfon M, Zeng H, Urano F, Till J, Hubbard S, Harding H, Clark S & Ron D (2002) IRE1 couples endoplasmic reticulum load to secretory capacity by processing the XBP-1 mRNA. *Nature* 415: 1–6.
- Chen X, Shen J & Prywes R. (2002) The luminal domain of ATF6 senses endoplasmic reticulum (ER) stress and causes translocation of ATF6 from the ER to the Golgi. *J Biol Chem* 277: 13045-13052.
- Chen Z, Yu W & Strickland S. (2007) Peripheral regeneration. *Annu. Rev. Neurosci.* 30: 209-233.
- Cornejo V, Pihán P, Vidal R & Hetz C (2013) Role of the unfolded protein response in organ physiology: lessons from mouse models. *IUBMB Life* 65: 962–75.
- Court F & Coleman M. (2012) Mitochondria as a central sensor for axonal degenerative stimuli. *Trends Neurosci* 35: 364-372.
- D'Antonio M, Musner N, Scapin C, Ungaro D, Del Carro U, Ron D, Feltri M & Wrabetz L (2013) Resetting translational homeostasis restores myelination in Charcot-Marie-Tooth disease type 1B mice. *J. Exp. Med.* 210: 821–38.
- DenBoer L, Hardy-Smith P, Hogan M, Cockram G, Audas T & Lu R (2005) Luman is capable of binding and activating transcription from the unfolded protein response element. *Biochem. Biophys. Res. Commun.* 331: 113–9.

- Dioufa N, Chatzistamou I, Farmaki E, Papavassiliou A & Kiaris H. (2012) P53 Antagonizes the Unfolded Protein Response and Inhibits Ground Glass Hepatocyte Development During Endoplasmic Reticulum Stress. *Experimental biology and medicine* 237: 1173–1180.
- Dubový P. (2011) Wallerian degeneration and peripheral nerve conditions for both axonal regeneration and neurophatic pain induction. *Ann. Ana.* 193:267-275.
- Fancy S, Chan J, Baranzini S, Franklin R & Rowitch D. (2011) Myelin regeneration: a recapitulation of development? *Annu Rev Neurosci* 34: 21-43.
- Fawcett J & Keynes R. (1990) Peripheral nerve regeneration. *Annu. Rev. Neurosci.* 13: 43-60.
- Ferguson T & Son Y. (2011) Extrinsic and intrinsic determinants of nerve regeneration. *J Tissue Eng* 2: 2041731411418392.
- Gaudet A, Popovich P & Ramer M. (2011) Wallerian degeneration: Gaining perspective on inflammatory events after peripheral nerve injury. *J Neuroinflammation.* 8: 110.
- Glenn T & Talbot W. (2013) Signals regulating myelination in peripheral nerves and the Schwann cell response to injury. *Curr Opin Neurobiol* 23: 1041-1048.
- Han H, Myllykoski M, Ruskamo S, Wang C & Kursula P. (2013) Myelin-specific proteins: a structurally diverse group of membrane-interacting molecules. *Biofactors* 39: 233-241.
- Harding H, Novoa I, Zhang Y, Zeng H, Wek R, Schapira M & Ron D. (2000) Regulated translation initiation controls stress-induced gene expression in mammalian cells. *Mol Cell* 6: 1099-1108.
- Harding H, Zhang Y, Zeng H, Novoa I, Lu P, Calton M, Sadri N, Yun C, Popko B, Paules R, Stojdl D, Bell J, Hettmann T, Leiden J & Ron D. (2003) An integrated stress response regulates amino acid metabolism and resistance to oxidative stress. *Molecular Cell* 11: 619-633.
- Hayashi A, Kasahara T, Iwamoto K, Ishiwata M, Kametani M, Kakiuchi C, Furuichi T & Kato T. (2007) The Role of Brain-derived Neurotrophic Factor (BDNF)-induced XBP1 Splicing during Brain Development 282: 34525-34534.
- Haze K, Yoshida H, Yanagi H, Yura T & Mori K. (1999) Mammalian transcription factor ATF6 is synthesized as a transmembrane protein and activated by proteolysis in response to endoplasmic reticulum stress. *Mol Biol Cell* 10: 3787-3799.
- Hetz C, Lee A, Gonzalez-Romero D, Thielen P, Soto C & Glimcher L. (2008) Unfolded protein response transcription factor XBP-1 does not influence prion replication or pathogenesis. *Proc Natl Acad Sci* 105: 757-762.
- Hetz C, Thielen P, Matus S, Nassif M, Court F, Kiffin R, Brown R, Glimcher L, Martinez G & Mari A (2009) XBP-1 deficiency in the nervous system protects against amyotrophic lateral sclerosis by increasing autophagy. 23: 2294–2306.
- Hetz C, Martinon F, Rodriguez D & Glimcher L. (2011) The unfolded protein response: integrating stress signals through the stress sensor IRE1 α . *Physiological reviews* 91: 1219–1243.
- Hetz C. (2012) The unfolded protein response: controlling cell fate decisions under ER stress and beyond. *Nat Rev Mol Cell Biol* 13: 89-102.
- Hetz C, Chevet E & Harding H (2013) Targeting the unfolded protein response in disease. *Nat. Rev. Drug Discov.* 12: 703–19.

- Hetz C & Mollereau B. (2014) Disturbance of endoplasmic reticulum proteostasis in neurodegenerative diseases. *Nat Rev Neurosci* 15: 233-249.
- Hirata, K. and Kawabuchi, M. (2002) Myelin phagocytosis by macrophages and nonmacrophages during Wallerian degeneration. *Microscopy research and technique* 57(6): 541-547.
- Hu, Y., Park, K., Yang, L., Wei, X., Yang, Q., Cho, K., Thielen, P., Lee, A., Cartoni, R., Glimcher, L., Chen, D. and He, Z. (2012) Differential effects of unfolded protein response pathways on axon injury-induced death of retinal ganglion cells. *Neuron* 73(3): 445-52.
- Huh, W., Esen, E., Geahlen, J., Bredemeyer, A., Lee, A., Shi, G., Konieczny, S., Glimcher, L. and Mills J. (2010) XBP1 controls maturation of gastric zymogenic cells by induction of MIST1 and expansion of the rough endoplasmic reticulum. *Gastroenterology* 139(6): 2038-2049
- Jessen, K. and Mirsky, R. (2008) Negative regulation of myelination: relevance for development, injury, and demyelinating disease. *Glia* 56: 1552-1565.
- Inserra, M., Bloch, D. and Terris, D. (1998) Functional indices for sciatic, peroneal, and posterior tibial nerve lesions in the mouse. *Microsurgery* 18(2): 119-24.
- Iwakoshi, N., Lee A., Vallabhajosyula, P., Otipoby K., Rajewsky K. and Glimcher, L. (2003) Plasma cell differentiation and the unfolded protein response intersect at the transcription factor XBP-1. *Nature Immunology* 4(4): 321-329.
- Jung H, Yoon B & Holt C (2012) Axonal mRNA localization and local protein synthesis in nervous system assembly, maintenance and repair. *Nat. Rev. Neurosci.* 13: 308-324
- Kozutsumi, Y., Segal, M., Normington, K., Gerhing, M. and Sambrook, J. (1988) The presence of malformed proteins in the endoplasmic reticulum signals the induction of glucose-regulated proteins. *Nature* 332(6163): 462-464.
- Lee A, Iwakoshi N & Glimcher L (2003) XBP-1 regulates a subset of endoplasmic reticulum resident chaperone genes in the Unfolded Protein Response. *Mol. Cell. Biol.* 23: 7448-7459.
- Lee, A., Chu, G., Iwakoshi, N. and Glimcher, L. (2005) XBP-1 is required for biogenesis of cellular secretory machinery of exocrine glands. *EMBO Journal* 24(24): 4368-4380.
- Lee K, Tirasophon W, Shen X, Michalak M, Prywes R, Okada T, Yoshida H, Mori K & Kaufman RJ (2002) IRE1-mediated unconventional mRNA splicing and S2P-mediated ATF6 cleavage merge to regulate XBP1 in signaling the unfolded protein response. *10*: 452-466.
- Li S, Yang L & Selzer ME (2013) Neuronal endoplasmic reticulum stress in axon injury and neurodegeneration. *Ann. Neurol.* 74: 768-777.
- Liang G, Audas T, Li Y, Cockram G, Dean J, Martyn A, Kokame K & Lu R (2006) Luman/CREB3 induces transcription of the endoplasmic reticulum (ER) stress response protein Herp through an ER stress response element. *Mol. Cell. Biol.* 26: 7999-8010.
- Lin, W. and Popko, B. (2009) Endoplasmic reticulum stress in disorders of myelinating cells. *Nature Neuroscience* 12(4): 379-385.
- Lutz AB & Barres BA (2014) Contrasting the glial response to axon injury in the central and peripheral nervous systems. *Dev. Cell* 28: 7-17.

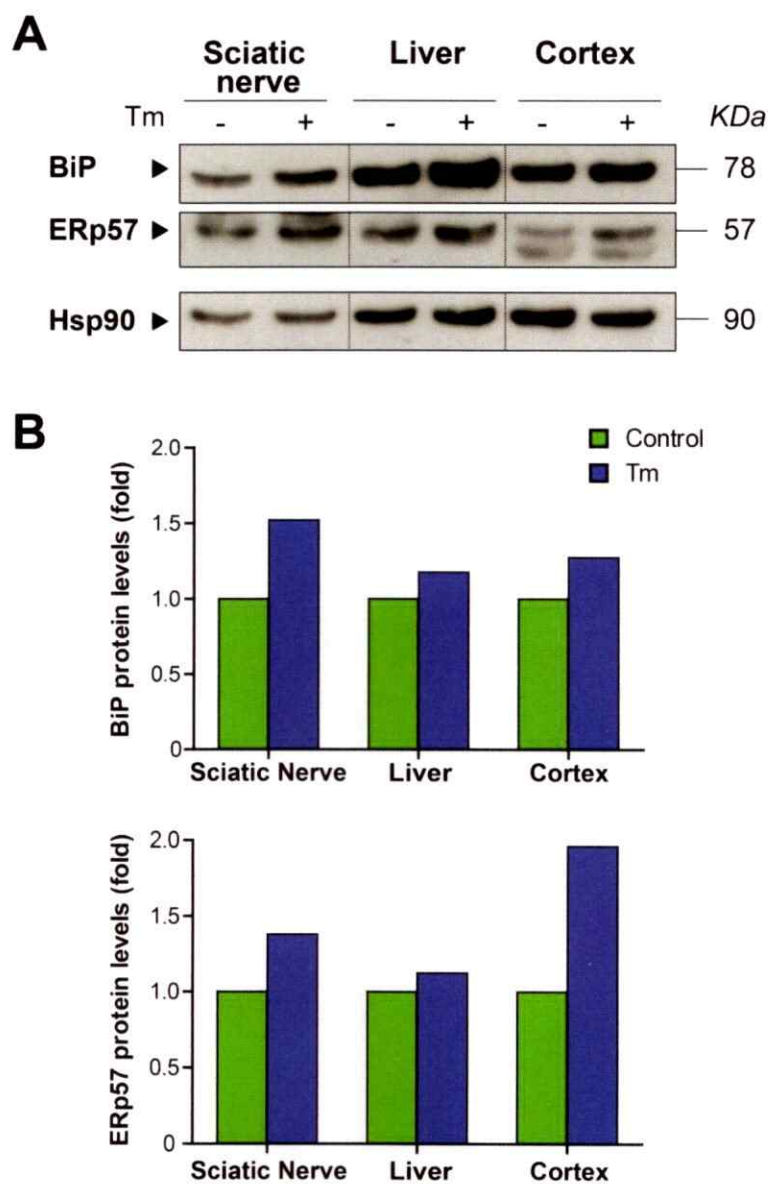
- Madduri, S. and Gander, B. (2010) Schwann cell delivery of neurotrophic factors for peripheral nerve regeneration. *J Peripher Nerv Syst* 15(2): 93-103.
- Mahadevan, N., Rodvold, J., Sepulveda, H., Rossi, S., Drew, A. and Zanetti, M. (2011) Transmission of endoplasmic reticulum stress and pro-inflammation from tumor cells to myeloid cells. *Proc. Natl Acad. Sci.* 108 (16) 6561–6566.
- Mahadevan, N., Anufreichik, V., Rodvold, J., Chiu, K., Sepulveda, H. and Zanetti, M. (2012) Cell-extrinsic effects of tumor ER stress imprint myeloid dendritic cells and impair CD8+ T cell priming. *PLoS One* 7(12): e51845.
- Mantuano, E., Henry, K., Yamauchi, T., Hiramatsu, N., Yamauchi, K., Orita, S., Takahashi, K., Lin, J., Gonias, S. and Campanam, W. (2011) The unfolded protein response is a major mechanism by which LRP1 regulates Schwann cell survival after injury. *The Journal of neuroscience* 31(38): 13376–13385.
- Martinon F & Glimcher LH (2011) Regulation of innate immunity by signaling pathways emerging from the endoplasmic reticulum. *Curr. Opin. Immunol.* 23: 35–40.
- Masuoka HC & Townes TM (2002) Targeted disruption of the activating transcription factor 4 gene results in severe fetal anemia in mice. *Blood* 99: 736–745.
- Matus S, Lopez E, Valenzuela V, Nassif M & Hetz C (2013) Functional contribution of the transcription factor ATF4 to the pathogenesis of amyotrophic lateral sclerosis. *PLoS One* 8: e66672.
- Maurel M, Chevet E, Tavernier J & Gerlo S (2014) Getting RIDD of RNA: IRE1 in cell fate regulation. *Trends Biochem. Sci.* 39: 245–54.
- Moreno J a, Halliday M, Molloy C, Radford H, Verity N, Axten JM, Ortori C a, Willis AE, Fischer PM, Barrett D a & Mallucci GR (2013) Oral treatment targeting the Unfolded Protein Response prevents neurodegeneration and clinical disease in prion-infected mice. *Sci. Transl. Med.* 5: 206ra138
- Moreno JA, Radford H, Peretti D, Steinert JR, Verity N, Martin MG, Halliday M, Morgan J, Dinsdale D, Catherine A, Barrett DA, Tsayler P, Bertolotti A, Willis AE & Mallucci GR (2012) Sustained translational repression by eIF2 α -P mediates prion neurodegeneration. *Nature* 485: 507–511.
- Ohri SS, Maddie M a, Zhang Y, Shields CB, Hetman M & Whittemore SR (2012) Deletion of the pro-apoptotic endoplasmic reticulum stress response effector CHOP does not result in improved locomotor function after severe contusive spinal cord injury. *J. Neurotrauma* 29: 579–88.
- Ohri SS, Hetman M & Whittemore SR (2013) Restoring endoplasmic reticulum homeostasis improves functional recovery after spinal cord injury. *Neurobiol. Dis.* 58: 29–37.
- Ohri SS, Mullins A, Hetman M & Whittemore SR (2014) Inhibition of GADD34, the Stress-Inducible Regulatory Subunit of the Endoplasmic Reticulum Stress Response, Does Not Enhance Functional Recovery after Spinal Cord Injury. *PLoS One* 9: e109703.
- Patzig J, Jahn O, Tenzer S, Wichert SP, de Monasterio-Schrader P, Rosfa S, Kuharev J, Yan K, Bormuth I, Bremer J, Aguzzi A, Orfaniotou F, Hesse D, Schwab MH, Möbius W, Nave K-A & Werner HB (2011) Quantitative and integrative proteome analysis of peripheral nerve myelin identifies novel myelin proteins and candidate neuropathy loci. *J. Neurosci.* 31: 16369–86.
- Penas, C., Font-Nieves, M., Forés, J., Petegnief, V., Planas, A., Navarro, X. and Casas, C. (2011) Autophagy, and BiP level decrease are early key events in retrograde degeneration of motoneurons. *Cell death and differentiation* 18(10): 1617–27.

- Pennuto, M., Tinelli, E., Malaguti, M., Del Carro, U., D'Antonio, M., Ron, D., Quattrini, A., Feltri, M. and Wrabetz, L. (2008) Ablation of the UPR-mediator CHOP restores motor function and reduces demyelination in Charcot-Marie-Tooth 1B mice. *Neuron* 57(3): 393–405.
- Pereira, J., Lebrun-Julien, F. and Suter, U. (2012) Molecular mechanisms regulating myelination in the peripheral nervous system. *Trends Neuroscience* 35(2): 123-134.
- Quarles, R. (2002) Myelin sheaths: glycoproteins involved in their formation, maintenance and degeneration. *Cell and Molecular Life Sciences* 59(11): 1851–1871.
- Ramírez O & Couve A (2011) The endoplasmic reticulum and protein trafficking in dendrites and axons. *Trends Cell Biol.* 21: 219–27.
- Reimold, A., Iwakoshi, N., Manis, J., Vallabhajosyula, P., Szomolanyi-Tsuda, E., Gravalles, E., Friend, D., Grusby, M., Alt, F. and Glimcher, L. (2001) Plasma cell differentiation requires the transcription factor XBP-1. *Nature* 412(6844): 300-307.
- Richardson, C., Kooistra, T. & Kim, D. (2010) An essential role for XBP-1 in host protection against immune activation in *C. elegans*. *Nature* 25(463): 1092–1095.
- Rishal I & Fainzilber M (2014) Axon-soma communication in neuronal injury. *Nat Rev Neurosci* 15: 32-42.
- Rodriguez, D., Zamorano, S., Lisbona, F., Rojas-Rivera, D., Urra, H., Cubillos-Ruiz, J., Armisen, R., Henriquez, D., Cheng, E., Letek, M., Vaisar, T., Irrazabal, T., Gonzalez-Billault, C., Letai, A., Pimentel-Muñoz, F., Kroemer, G. and Hetz, C. (2012) BH3-only proteins are part of a regulatory network that control the sustained signalling of the unfolded protein response sensor IRE1 α . *EMBO Journal* 31(10): 2322-2335.
- Salzer, J. (2012) Axonal regulation of Schwann cell ensheathment and myelination. *J Peripher Nerv Syst* 3:14-19.
- Saxena, S., Cabuy, E. and Caroni, P. (2009) A role for motoneuron subtype-selective ER stress in disease manifestations of FALS mice. *Nature neuroscience* 12(5): 627–36.
- Schröder, M. and Keufman, R. (2005) The mammalian unfolded protein response. *Annu Rev Biochem* 74: 739-789.
- Shen X, Ellis RE, Lee K, Liu C, Yang K, Solomon A, Yoshida H, Morimoto R, Kurnit DM, Mori K, Kaufman RJ & Arbor A (2001) Complementary signaling pathways regulate the Unfolded Protein Response and are required for *C. elegans* development. 107: 893–903.
- Shoulders, M., Ryno, L., Genereux, J., Moresco, J., Tu, P., Wu, C., Yates, J., Su, A., Kelly, J. and Wiseman, R. (2013) Stress-independent activation of XBP1s and/or ATF6 reveals three functionally diverse ER proteostasis environments. *Cell Rep* 3: 1279-1292.
- Sofroniew M V (2009) Molecular dissection of reactive astrogliosis and glial scar formation. *Trends Neurosci.* 32: 638–647.
- Stoll, G., Jander, S. and Myers, R. (2002) Degeneration and regeneration of the peripheral nervous system: From Augustus Waller's observations to neuroinflammation. *Journal of the Peripheral Nervous System* 7(1): 13–27.
- Tabas I & Ron D (2011) Integrating the mechanisms of apoptosis induced by endoplasmic reticulum stress. *Nat. Cell Biol.* 13: 184–190.

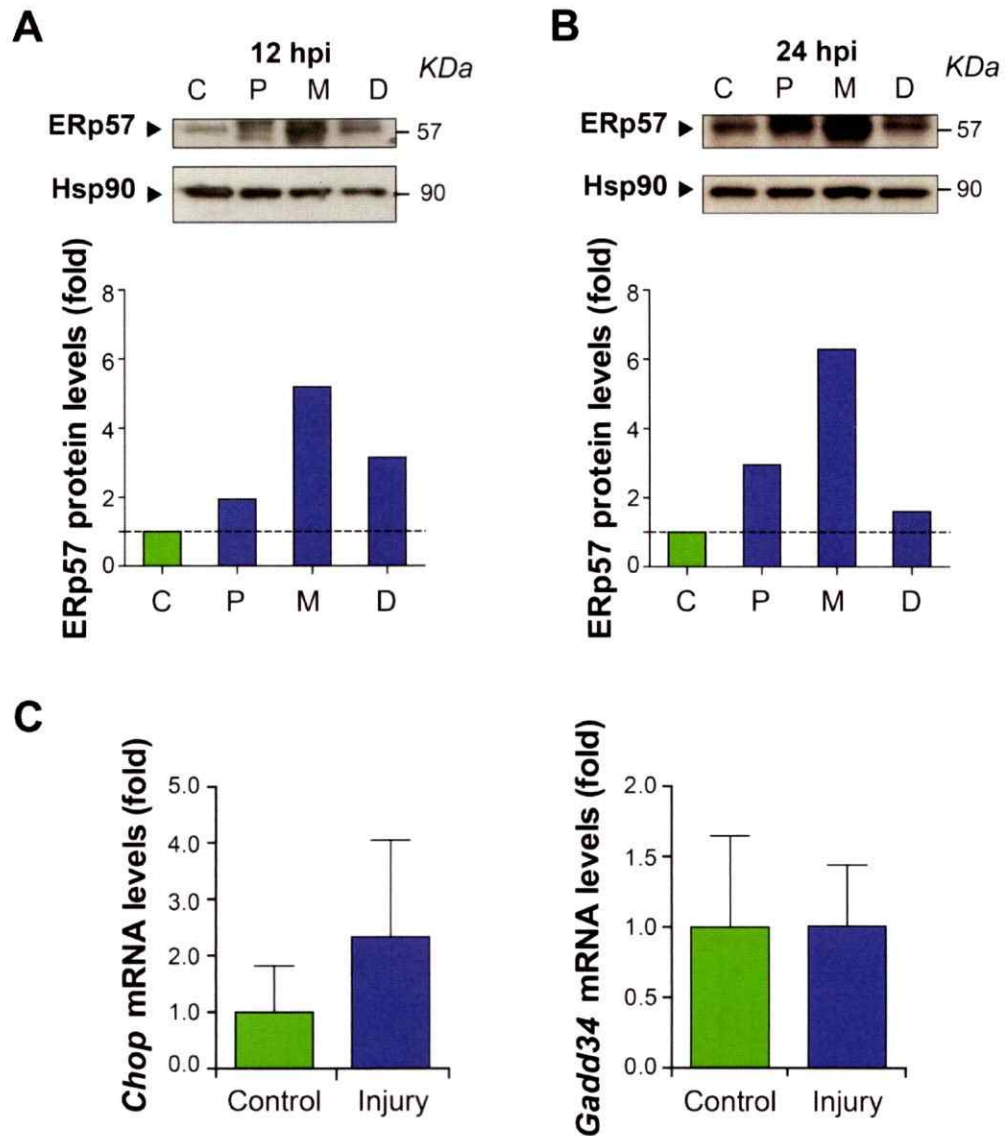
- Taylor, R. and Dillin, A. (2013) XBP -1 is a cell-nonautonomous regulator of stress resistance and longevity. *Cell* **153**(7): 1435–1447.
- Taylor R., Berendzen, K. and Dillin, A. (2013) Systemic stress signalling: understanding the cell non-autonomous control of proteostasis. *Nature Reviews. Molecular Cell Biology* **15**(3): 211-217.
- Tofaris GK, Patterson PH, Jessen KR & Mirsky R (2002) Denervated Schwann Cells Attract Macrophages by Secretion of Leukemia Inhibitory Factor (LIF) and Monocyte Chemoattractant Protein-1 in a Process Regulated by Interleukin-6 and LIF. *J. Neurosci.* **22**: 6696–6703.
- Toy, D. and Namgung, U. (2013) Role of glial cells in axonal regeneration. *Exp Neurobiology* **22**(2):68-76.
- Tsang, Kl., Chan, D., Cheslett, D., Chan, W., Leong So, C., Melhado, U., Chan T., Kwan, K., Hunziker, E., Yamada, Y., Bateman, J., Cheung, K. and Cheah, K. (2007) Surviving Endoplasmic Reticulum Stress Is Coupled to Altered Chondrocyte Differentiation and Function. *PLoS Biology* **5**(3): e44.
- Urrea H, Dufey E, Lisbona F, Rojas-Rivera D & Hetz C (2013) When ER stress reaches a dead end. *Biochim. Biophys. Acta* **1833**: 3507–17.
- Valdés P, Mercado G, Vidal RL, Molina C, Parsons G, Court F a, Martinez A, Galleguillos D, Armentano D, Schneider BL & Hetz C (2014) Control of dopaminergic neuron survival by the unfolded protein response transcription factor XBP1. *PNAS* **111**: 6804–9.
- Valenzuela, V., Collyer, E., Armentano, D., Parsons, G., Court, F. and Hetz, C. (2012) Activation of the unfolded protein response enhances motor recovery after spinal cord injury. *Cell death & disease* **3**(2): e272.
- Vargas, M. and Barres, B. (2007) Why is Wallerian degeneration in the CNS so slow?. *Annu. Rev. Neurosci.* **30**:153-179.
- del Vecchio C a, Feng Y, Sokol ES, Tillman EJ, Sanduja S, Reinhardt F & Gupta PB (2014) De-differentiation confers multidrug resistance via noncanonical PERK-Nrf2 signaling. *PLoS Biol.* **12**: e1001945.
- Vidal R, Figueroa A, Court F, Thielen P, Molina C, Wirth C, Caballero B, Kiffin R, Segura-Aguilar J, Cuervo AM, Glimcher L & Hetz C (2012) Targeting the UPR transcription factor XBP1 protects against Huntington's disease through the regulation of FoxO1 and autophagy. *Hum. Mol. Genet.* **21**: 2245–2262.
- Villegas R, Martinez NW, Lillo J, Pihan P, Hernandez D, Twiss JL & Court FA (2014) Calcium release from intra-axonal endoplasmic reticulum leads to axon degeneration through mitochondrial dysfunction. *J. Neurosci.* **34**: 7179–89.
- Walter, P. and Ron, D. (2011) The unfolded protein response: from stress pathway to homeostatic regulation. *Science* **334**(6059): 1081-1086.
- Waller A (1850) Experiments on the section of the glossopharyngeal and hypoglossal nerves of the frog, and observations of the alterations produced thereby in the structure of their primitive fibres. *Philos. Trans. R. Soc. B Biol. Sci.* **140**: 423–429.
- Wang, J., Medress, Z. and Barres, B. (2012) Axon degeneration: Molecular mechanisms of a self-destruction pathway. *J Cell Biol* **196**(1): 7-18.

- White, J., Smithwick, R., and Simeone, F. (1952). The autonomic nervous system. *The American Journal of Nursing*, 52(11): 1394.
- Yao, D., Li, M., Shen, D., Ding, F., Lu, S., Zhao, Q. and Gu, X. (2013) Expression changes and bioinformatic analysis of Wallerian degeneration after sciatic nerve injury in rat. *Neuroscience Bulletin* 29(3): 321-332.
- Ying Z, Misra V & Verge V (2014) Sensing nerve injury at the axonal ER: Activated Luman/CREB3 serves as a novel axonally synthesized retrograde regeneration signal. *PNAS* 111: 16142–7.
- Yoshida H, Matsui T, Yamamoto A, Okada T & Mori K (2001) XBP1 mRNA is induced by ATF6 and spliced by IRE1 in response to ER stress to produce a highly active transcription factor. *Cell* 107: 881–891.
- Zhang, J., Luo, X., Xian, C., Liu, Z. and Zhou, X. (2008) Endogenous BDNF is required for myelination and regeneration of injured sciatic nerve in rodents. *European Journal of Neuroscience* 12(12): 4171-4180.
- Zhang, K. and Kaufman, R. (2008) Identification and Characterization of Endoplasmic Reticulum Stress-Induced Apoptosis In Vivo. *Methods in Enzymology* 442: 395–419.
- Zhang, K., Wong, H., Song, B., Miller, C., Scheuner, D. and Kaufman, R. (2005) The unfolded protein response sensor IRE1 α is required at 2 distinct steps in B cell lymphopoiesis. *The Journal of Clinical Investigation* 115(2): 268-281.
- Zhang H, Zhang X, Wang Z, Shi H, Wu F, Lin B, Xu X, Wang X, Fu X, Li Z, Shen C, Li X & Xiao J (2013) Exogenous basic fibroblast growth factor inhibits ER stress-induced apoptosis and improves recovery from spinal cord injury. *CNS Neurosci. Ther.* 19: 20–9.
- Zhang H, Wu F, Kong X, Yang J, Chen H, Deng L, Cheng Y, Ye L, Zhu S, Zhang X, Wang Z, Shi H, Fu X, Li X, Xu H, Lin L & Xiao J (2014) Nerve growth factor improves functional recovery by inhibiting endoplasmic reticulum stress-induced neuronal apoptosis in rats with spinal cord injury. *J. Transl. Med.* 12: 130.
- Zuleta A, Vidal R, Armentano D, Parsons G & Hetz C (2012) AAV-mediated delivery of the transcription factor XBP1s into the striatum reduces mutant Huntingtin aggregation in a mouse model of Huntington's disease. *Biochem. Biophys. Res. Commun.* 420: 558–63.

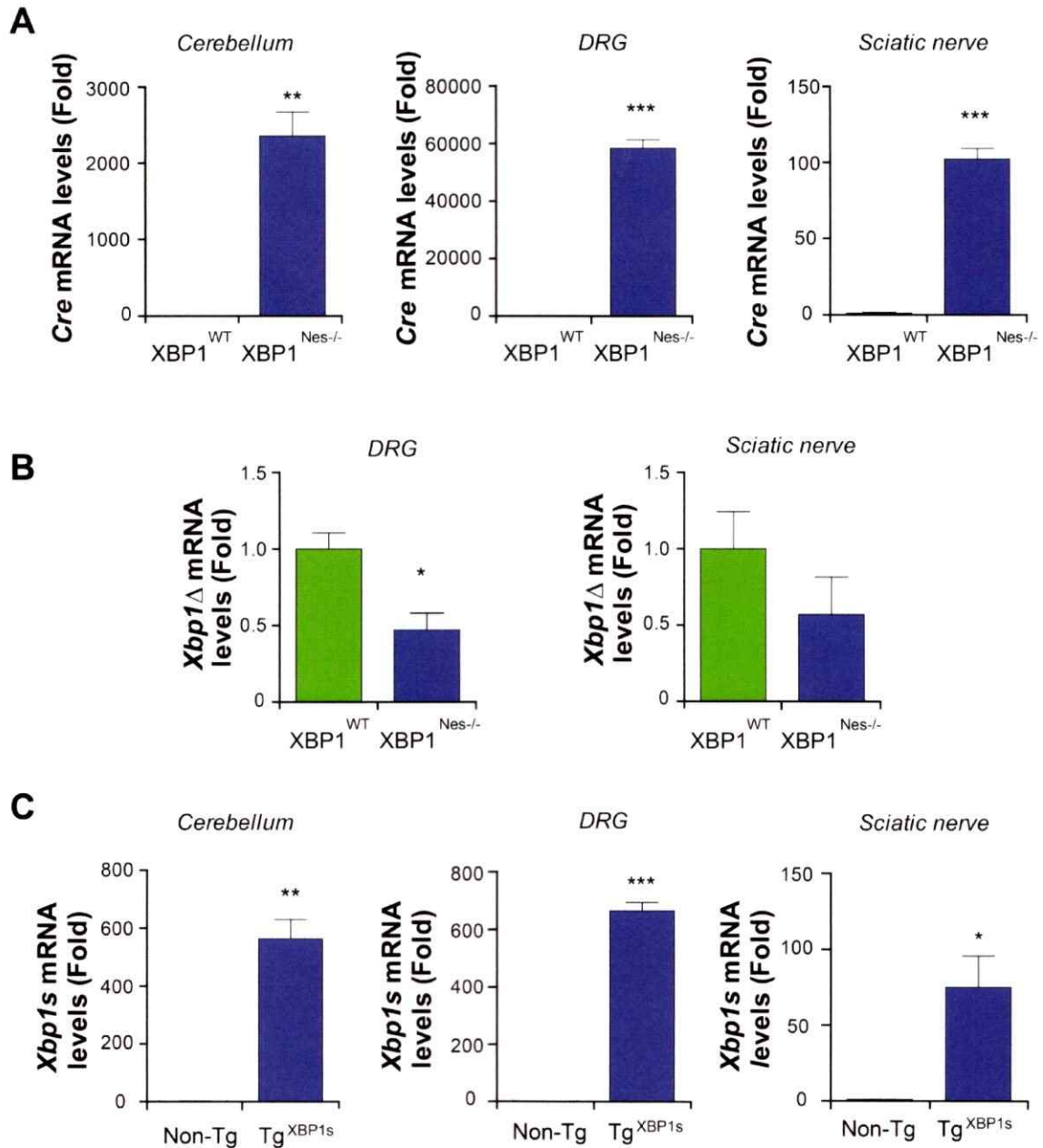
11. Supplementary data



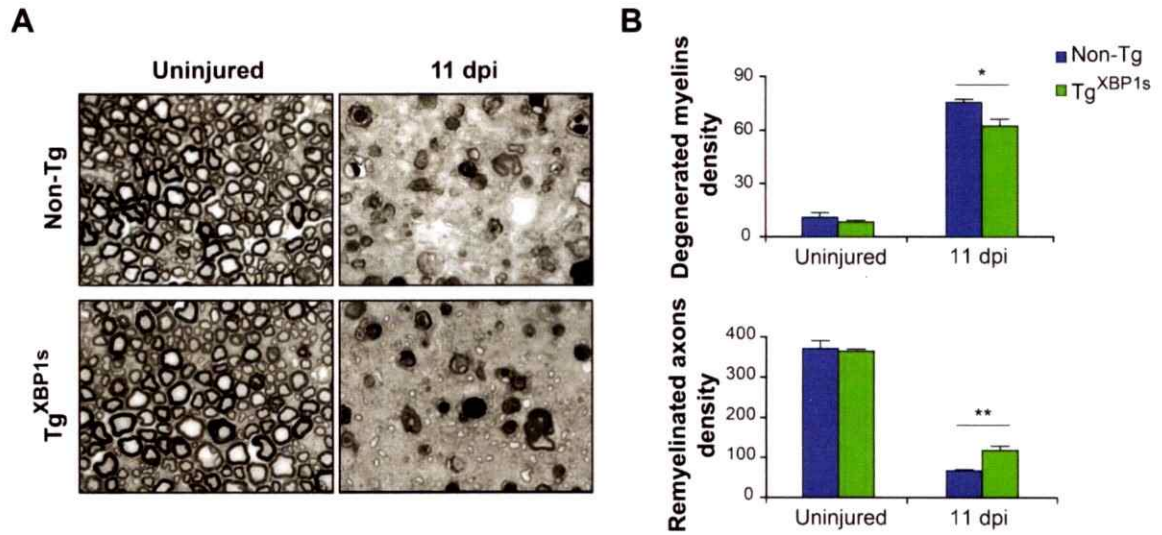
Supplementary Figure S1. Pharmacological UPR activation in sciatic nerve. (A) WT mice were intraperitoneally injected with Tm or DMSO. After 16 hours, sciatic nerve, liver and brain cortex were extracted for protein expression analysis. The ER chaperones BiP and ERp57 were evaluated and (B) quantified by densitometry, normalized against the loading control Hsp90 and compared with control treatments with DMSO.



Supplementary Figure S2. Sciatic nerve damage triggers UPR activation. WT mice were injured and at different days post-injury (dpi) a 5 mm region of the sciatic nerve was removed in the injured region (medial, M) and adjacent proximal (P) and distal (D) for posterior analysis. ERp57 protein levels were evaluated at **(A)** 12 and **(B)** 24 hours post injury (hpi). **(C)** *Chop* and *Gadd34*, expression was analyzed from sciatic nerves by real-time PCR in uninjured conditions and at 2 dpi in distal nerve regions. For C), data are expressed as mean \pm S.E.M.; Student's t-test; n = 3 animals per group.



Supplementary Figure S3. *Cre*, *Xbp1Δ* and *Xbp1s* mRNA expression in XBP1^{Nes-/-} and Tg^{XBP1s} mice, respectively. (A) *Cre* recombinase expression was analyzed in cerebellum, DRGs and sciatic nerves of XBP1^{Nes-/-} and XBP1^{WT} mice by real-time PCR in uninjured conditions. (B) The deleted exon II of the *Xbp1* gene was measured by real time PCR in DRGs and sciatic nerves of XBP1^{Nes-/-} and XBP1^{WT} mice by real-time PCR in uninjured conditions. (C) *Xbp1s* mRNA expression was analyzed by real-time PCR in Tg^{XBP1s} and non-Tg mice in uninjured conditions. Data are shown as mean ± S.E.M.; *, $p < 0.05$; **, $p < 0.01$; *, $p < 0.001$. Statistical differences were analyzed by student's t-test; $n = 3$ animals per group.**



Supplementary Figure S4. Overexpression of XBP1s increases myelin removal and axonal regeneration at 11 days after injury. (A) Tg^{XBP1s} and non-Tg mice were injured in the sciatic nerve and 11 days after damage nerves were extracted and stained with toluidine blue. Uninjured nerves were used as control. Transversal sections of distal region were analyzed for degenerated myelins and remyelinated fibers. (B) Quantification of degenerated myelins and remyelinated fibers showed in A. Data are shown as mean \pm S.E.M. * $p < 0.05$. Data were analyzed by two-way ANOVA followed by Bonferroni post test; $n = 3$ animals per group.